



Published in final edited form as:

*J Neuroendocrinol.* 2019 August ; 31(8): e12762. doi:10.1111/jne.12762.

## Gonadal hormones differentially regulate sex-specific stress effects on glia in medial prefrontal cortex

J.L. Bollinger<sup>1,2,3</sup>, I. Salinas<sup>3</sup>, E. Fender<sup>1</sup>, D.R. Sengelaub<sup>1,2,3</sup>, C.L. Wellman<sup>1,2,3</sup>

<sup>1</sup>Department of Psychological and Brain Sciences, Indiana University, Bloomington IN

<sup>2</sup>Program in Neuroscience, Indiana University, Bloomington IN

<sup>3</sup>Center for the Integrative Study of Animal Behavior, Indiana University, Bloomington IN

### Abstract

Women are more susceptible to various stress-linked psychopathologies, including depression. Dysfunction of medial prefrontal cortex (mPFC) has been implicated in depression, and studies indicate sex differences in stress effects on mPFC structure and function. For instance, chronic stress induces dendritic atrophy in mPFC in male rats, yet dendritic growth in females. Recent findings suggest glial pathways toward depression. Glia are highly responsive to neuronal activity, and function as critical regulators of synaptic plasticity. Preclinical models demonstrate stress-induced microglial activation in mPFC in males, yet deactivation in females. In contrast, stress reduces astrocyte complexity in mPFC in male rats; effects in females are unknown. Glia possess receptors for most gonadal hormones, and gonadal hormones are known to modulate neuronal activity. Thus, gonadal hormones represent a potential mechanism underlying sex differences in- and divergent stress effects on- glia. Therefore, we examined the role of gonadal hormones in sex-specific stress effects on neuronal activity (i.e. FosB/ FosB induction) and glia in mPFC. Findings indicate greater microglial activation in mPFC in females, and greater astrocyte area in males. Basal astrocyte morphology is modulated by androgens, whereas androgens or estrogens dampen microglial state in males. Astrocyte morphology is associated with neuronal activity in both sexes, regardless of hormonal condition. Chronic stress induced astrocytic atrophy in males, yet hypertrophy in females; gonadal hormones, in part, regulate this difference. Stress effects on microglia are estradiol-dependent in females. Together, these data suggest sex-specific, gonadal hormone-dependent stress effects on astrocytes and microglia in mPFC.

### Keywords

Astroglia; Depression; Estradiol; Microglia; Testosterone

---

Corresponding Author: Cara L. Wellman, wellmanc@indiana.edu, 812-855-4922, Indiana University, 1101 E. 10<sup>th</sup> St. Bloomington, IN, 47405.

Conflict of Interest Statement: The authors declare no competing financial interests.

## Introduction

Women are twice as likely to suffer from depression and three times as likely to experience a depressive episode following a stressful life event (1, 2). This sex discrepancy emerges around puberty, widens over adolescence, remains through adulthood, and disappears with menopause (3–5), suggesting that estrogens may enhance susceptibility to depression. In contrast, androgens may play a protective role in men, as lower levels of testosterone (T) and genetic polymorphisms associated with reduced efficiency of transcription of the androgen receptor (AR) increase risk for depression in aged males (6, 7).

Dysfunction of medial prefrontal cortex (mPFC), among other brain regions, has been implicated in numerous stress-linked disorders, including depression, and animal studies indicate sex-specific stress effects on mPFC structure and corticolimbic function. For instance, male and female rats show opposite patterns of stress-induced dendritic remodeling in mPFC: chronic stress decreases apical dendritic branch length in pyramidal cells in males, but either has no effect on (8) or increases (9) dendritic length in females. Estradiol (E) is necessary for stress-induced dendritic hypertrophy in females (9, 10).

Likewise, chronic stress alters microglial morphology, function, and microglia-neuron interaction in mPFC in a sex-specific manner (11, 12). Microglia are the immunocompetent cells of the brain and are capable of modeling and refining neural tissue through the release of neurotrophic factors, cytokines, and chemokines, engagement with complement proteins, and direct microglia-neuron contact. These cells can modulate neuronal activity, prune synapses, and alter behavioral function (reviewed in 13, 14). Many of these actions appear to be sex-, region-, and hormone-dependent (15–17). In fact, prior exposure to gonadal hormones and local cues from the microenvironment establish sex- and region- specific microglial transcriptomes (18, 19).

We recently demonstrated a basal sex difference in microglial morphology in mPFC in adult rats, and dramatic sex-dependent stress effects on microglial morphology and immune factor expression (11). Microglia in mPFC in unstressed females exhibit a more activated profile compared to males. Remarkably, chronic stress has either no effect on- or induces- microglial morphological activation in mPFC in males (20, 21), but decreases morphological activation in females (11). Estradiol plays a role in microglial differentiation (15). Estrogen receptors (ERs) are expressed on microglia, and injury induces expression of microglial ARs (22, 23). Thus, gonadal hormones could mediate sex differences in adult microglial state and stress reactivity.

Chronic stress also alters astrocyte complexity and physiology in mPFC in males (24). Astrocytes play a critical role in regulating synaptic stability and neurotransmission, and are important in glucagon storage, glucose homeostasis, and provide metabolic support to neurons (25). Astrocytic processes surround synapses and are directly juxtaposed against neuronal elements. By modulating neuronal function, these cells can influence behavior and may be an important driver of stress effects on brain architecture and function (26). Moreover, astrocytes produce numerous microglia-relevant signals, including glutamate,

purines, complement proteins, cytokines, and chemokines (27). As such, multiple glial signaling cascades likely contribute to the complex effects of stress on brain and behavior.

Chronic stress reduces astrocyte complexity in mPFC in males (28), and this contributes to stress-induced reductions in astrocyte-astrocyte gap junctions (29), and the slowing of astrocyte metabolism (30). These alterations might contribute to stress-linked depressive-like behaviors: experimentally induced reductions in astrocyte number and complexity in mPFC cause depressive-like behaviors similar to those seen after stress (31).

Although sparsely investigated, findings indicate sex differences in astrocyte density and morphology across a number of stress-sensitive brain regions. For instance, males show heightened astrocyte density and complexity in medial amygdala (32), whereas astrocytic complexity in hippocampus is greater in females (33). Astrocytes express ARs and ERs (34, 35), alongside factors critical in steroidogenesis and steroid aromatization (36, 37). Therefore, astrocytes are capable of both receiving input from gonadal hormones and modulating the actions of gonadal steroids on neighboring cells. Taken together, these data suggest probable sex differences in- and sex-dependent stress effects on- astrocyte morphology in mPFC.

In addition to gonadal steroids, microglia and astrocytes are sensitive to neuronal signals, including glutamate (38). Chronic stress reduces glutamatergic signaling in pyramidal neurons in mPFC in males but not females (39), and stress-induced activation of glutamatergic neurons is associated with microglial remodeling in mPFC in males (21, 40). This relationship has yet to be examined in females. Therefore, we first investigated potential sex differences in chronic stress-induced neuronal activation (as assessed using FosB induction), astrocyte morphology, and the relationship between neuronal activation and glial complexity in mPFC; we then examined the role of gonadal hormones in stress-induced FosB induction, and sex specific glial remodeling in mPFC. Stress effects on neuronal morphology in mPFC are most often found in apical dendritic arbors. Therefore, we hypothesized that stress-induced glial remodeling will be localized to layers 1 and 2/3 in mPFC, as apical arbors predominate in these laminae. Moreover, we predicted a modulatory role for gonadal hormones in sex-dependent glial phenotypes and stress-linked glial alterations in mPFC.

## Methods

Two experiments were performed in tandem, investigating the role of gonadal hormones in stress-induced glial remodeling in 1) males and 2) females. Basal sex differences were examined in unstressed animals.

### Hormone Manipulations and Restraint Stress

Male and female Sprague-Dawley rats (79.93±0.23 days at start; Envigo, Indianapolis, IN) underwent sham gonadectomies with blank implants (SHAM), gonadectomies with blank implants (ovariectomy, OVX; orchidectomy, CAST), or gonadectomies with hormonal replacement (OVX+estradiol [E], OVX+dihydrotestosterone [DHT], CAST+testosterone [T], CAST+E; Fig 1A). Surgeries were performed under ketamine-xylazine anesthesia

(male: 80 mg/kg ketamine, 7 mg/kg xylazine; female: 64 mg/kg ketamine, 7 mg/kg xylazine). Ovariectomies were completed as described in Garrett and Wellman (9), with an empty 10 mm silastic capsule (1.57 mm i.d., 3.18 mm i.d., Dow Corning) or a capsule containing 17 $\beta$ -estradiol (10% E in cholesterol, Steraloids, Inc., Newport, RI) or DHT (30 mm, Steraloids, Inc.) implanted subcutaneously. E implants produce plasma titers slightly higher than those of cycling females in the proestrus phase (41). To assess the effect of androgens in females, capsules containing DHT – which has a higher affinity for AR's than does T and, unlike T, cannot be converted to E – were used. Orchidectomies were performed as described in Verhovshek and Sengelaub (42). T was administered through a subcutaneous, intrascapular silastic implant (45 mm) that produces normal, physiological levels of circulating T (Steraloids, Inc.; 43). E was administered as described above. All rats received a single dose of post-operative rimadyl (1.25 mg/kg). Rats were group-housed by sex, hormone, and stress condition in a temperature- and humidity-controlled vivarium (12 h light/dark cycle, lights on 0800 h). Food and water were provided *ad libitum*. All experimental procedures were performed during the light phase, carried out in accordance with the NIH Guide for the Care and Use of Laboratory Animals, and approved by the Bloomington Institutional Animal Care and Use Committee.

Five to seven days after surgery, rats were exposed to either 10 days of daily restraint or were left unhandled except for weighing ( $n = 5-9$  / group). All rats were weighed every other day. Stressed rats were restrained in a semi-cylindrical plastic tube in their home cage for 3 h/day, with the time of restraint unpredictably varied over the light cycle. This procedure produces significant increases in plasma corticosterone (44), dendritic reorganization (9, 44), and sex-dependent microglial remodeling in mPFC (11). Just prior to euthanasia, vaginal cytology was examined and estrous phase determined in all female rats (SHAM: D1,  $n = 2$ ; D2,  $n = 10$ ; P,  $n = 5$ ; OVX: D1,  $n = 14$ ; D2,  $n = 1$ ; OVX+E: D1,  $n = 1$ ; D2,  $n = 2$ ; P,  $n = 12$ ; E,  $n = 1$ ; OVX+DHT: D1,  $n = 13$ ; D2,  $n = 2$ ). After euthanasia, adrenals were dissected and weighed to verify the stress manipulation, with adrenal-weight-to-body-weight ratios and weight change compared across groups. To confirm hormone manipulations, bulbocavernosus/levator ani muscles (BC/LA, males) and uteri (females) were dissected and weighed, and organ-weight-to-body-weight ratios were compared across conditions. All animals were euthanized between 1030–1800 h, with stressed animals euthanized  $24.17 \pm 0.23$  h post-restraint. An anti-FosB (N-terminus) primary antibody that recognize both FosB and its splice variant, FosB, was used in this study. Accumulation of FosB is associated with repeated neuronal activation. The majority of FosB protein degrades 24 h post-stress, whereas FosB remains stable (40). Therefore, brains were extracted approximately 24-h post-restraint, to ensure that the immunohistochemical signal measured in this study largely reflects FosB expression

### Immunohistochemistry

Animals were overdosed with urethane and transcardially perfused with 0.1 M phosphate-buffered saline (PBS) followed by 4% paraformaldehyde (PFA) in PBS. Brains were removed, fixed, sectioned, and stained as described in Bollinger, Burns (11). Briefly, free-floating sections (44  $\mu$ m, 1:6 series) were incubated 48 h at 4°C with an antibody specific to ionized calcium-binding adaptor molecule-1 (Iba-1, 1:2000; #019–19741, Wako Chemicals

Inc., Richmond, VA) in 5% bovine serum albumin (BSA)+PBS with Triton X (PBST), glial fibrillary acidic protein (GFAP, 1:3000; #AB5804, EMD Millipore, Billerica, MA) in 5% normal goat serum (NGS)+PBST, or FosB (1:500; #SC-48, Santa Cruz Biotechnology, Dallas, TX; 1:4000; #AB184938, ABCAM, Cambridge, UK) in 5% NGS+PBST. Sections were incubated 1 h at room temperature with biotinylated secondary antibody (1:500, #BA-1000, Vector Laboratories Inc., Burlingame, CA) in 5% BSA+PBST or 2.5% NGS +PBST, followed by 1 h in ABC complex (Vector Laboratories Inc.). Immunoreactive cells were visualized using a nickel-intensified DAB reaction. An additional series was stained with cresyl echt violet to facilitate identification of prefrontal cortex. Alternate series from the same animals were used for glial and neuronal measures. A control series lacking primary antibody incubation showed no staining.

### Thresholding and Morphological Analysis of Microglia and Astrocytes

Visual inspection of the tissue demonstrated that immunostaining of microglial and astrocyte morphology was characteristic of the targeted cell types (Fig 1C). Cell morphology was assessed using standardized thresholding and skeleton analyses. To measure the area of Iba-1 immunoreactive (Iba-1+) and GFAP immunoreactive (GFAP+) material in mPFC, images were collected from each hemisphere of 4 sections per animal, equally spaced through the anterior-posterior axis of prefrontal cortex (PL; 45; Fig 1B). Forceps minor and layers 1, 2/3, and 5/6 of PL were identified and outlined in cresyl echt violet-stained sections using Stereo Investigator (MBF Bioscience Inc., Williston, VT) interfaced with a Nikon E80i microscope and MicroFire Model S99808 camera (Optronics, Goleta, CA; exposure time: 6.25 ms, gain: 20). These outlines were superimposed onto corresponding Iba-1+ and GFAP+ sections, with the forceps minor aligned to each hemisphere. For Iba-1+ images, the microscope focus was centered in the z-axis of the section; in GFAP+ tissue, images were focused on the top and bottom of each section sampled. Images across the rostral-caudal extent of PL were collected from each layer in both hemispheres of each section (Iba-1+ tissue: 8–16 images/layer; GFAP+ tissue: 16–32 images/layer). For each section the average luminance was maintained at  $195 \pm 5$  A.U. (Iba-1+ tissue) or  $230 \pm 5$  A.U. (GFAP+ tissue). All images were collected at a final magnification of  $1800\times$  with TIFF files stored at a resolution of  $1600\times 1200$  pixels. Using a semi-automated technique, all files were converted to 8-bit grayscale TIFF images, uniformly “Sharpened”, and thresholded in ImageJ (NIH; threshold: 0 – 110). This threshold was chosen to capture the maximum amount of immunoreactive material with minimal flaring. Contrast was enhanced to reduce flaring when needed. The total area of thresholded material was then analyzed using the ImageJ measure function. In addition to immunoreactive area, glial process complexity was examined (4–8 images/layer/animal) as described in Vollmer, Ghosal (46) and Ganguly, Thompson (47). The “Analyze Skeleton” plugin was used to calculate the number of branch points and branch length (Fig 1C). These measures were summed and normalized to the number of cells in each image. Cell counts per image are presented for GFAP analyses. To compute process complexity, number of branch points and branch length per cell were z-normalized relative to average layer 5/6 values in unstressed SHAM animals for each respective sex, summed, and divided by 2.

The measures used in this study characterize interconnected aspects of glial morphology. For instance, the area of immunoreactive glial material may reflect cell density, process complexity, process thickness, and/or soma size, and should thus be conceptualized as an aggregate measure. In fact, pilot analyses indicate a strong positive correlation between microglial morphological classification (i.e. another aggregate measure) and immunoreactive area, with increased immunoreactive area associating with increases in primed microglia (Supplementary Fig 1). As the majority of immunohistochemical signal detected in this study is associated with glial processes, we examined glial process complexity. Associations between cell density and morphological characteristics within microglia and astrocytes were examined using Pearson's correlation coefficients.

## Stereology

FosB immunoreactive ( FosB+) cells were identified and stereologically counted in layers 2/3 and 5/6 of PL using the optical fractionator method, and Stereo Investigator (900× magnification, Fig 1C). Both hemispheres of 4 sections corresponding to the same cresyl echt violet outlines previously mentioned were analyzed per animal. An average of  $922.16 \pm 24.20$  FosB+ cells (mean CE: 0.05) were counted per animal (grid size:  $300 \times 300$   $\mu\text{m}$ ; counting frame:  $50 \times 50$   $\mu\text{m}$ ). Guard zones were set with a centered-probe thickness of 10  $\mu\text{m}$ . Iba-1+ cells were visualized and counted using the same procedure at 1800× magnification. An average of  $656.42 \pm 14.71$  Iba-1+ cells (mean CE: 0.05) were counted per animal (grid size:  $300 \times 300$   $\mu\text{m}$ ; counting frame:  $125 \times 125$   $\mu\text{m}$ ). Estimated densities were calculated and analyzed for FosB+ and Iba-1+ cells.

## Statistics

All data were collected with the researcher blind to sex and experimental condition. Statistical tests were performed using IBM SPSS Statistics 24 (IBM Corp., Armonk, NY). Two-way repeated measures ANOVA (sex  $\times$  layer) were used to analyze basal sex differences in unstressed SHAM males and females. Two-way ANOVA (hormonal condition  $\times$  stress condition) was used for body and tissue weight analyses, and three-way repeated measures ANOVA (hormonal condition  $\times$  stress condition  $\times$  layer) was used for cellular analyses. Significant ANOVA results were followed by Fisher's protected LSD post-hoc comparisons. Relationships between microglial, astrocyte, and neuronal measures were examined using Pearson correlation coefficients. To maintain statistical power, analyses targeted main effects only. Thus, hormonal conditions were collapsed across stress groups to examine stress effects, whereas unstressed and stressed groups were collapsed to examine hormonal effects. Due to the large number of correlations, only statistically significant associations ( $p < .05$ ) are reported. Outliers more than  $\pm 2$  standard deviations from the mean were removed from all analyses per standard lab procedures (11, 48).

## Results

### Manipulation Verification: Body and Tissue Weight

Hormone manipulation was confirmed using BC/LA weight in males and uterine weight in females. BC/LA weight differed with hormonal condition ( $F_{(3,45)} = 320.84$ ,  $p < .001$ ) and stress ( $F_{(1,45)} = 7.92$ ,  $p < .01$ ). Stress effects on BC/LA weight varied across hormone

treatments ( $F_{(3,45)} = 5.70, p < .01$ ). Post-hoc comparisons indicate reduced BC/LA-weight-to-body-weight ratios in CAST and CAST+E males compared to SHAM and CAST+T animals, regardless of stress ( $p < .001$ , Fig 2A). BC/LA weight was slightly increased (17%) in CAST+T compared to SHAM males ( $p < .001$ ). Chronic stress had no effect on BC/LA weight in SHAM and CAST males, but induced a slight increase (12%) in BC/LA weight in CAST+T animals ( $p < .001$ ). Uterine-to-body-weight ratio differed with hormonal condition in females ( $F_{(3,71)} = 72.02, p < .001$ ). Post-hoc comparisons indicate reduced uterine weight in OVX compared to SHAM animals ( $p < .001$ ). Uterine weight was restored in OVX+E but not OVX+DHT females ( $p < .001$ ; Fig 2A). Stress did not affect uterine weight (effect of stress:  $F_{(1,71)} = 0.73, ns$ ; hormonal condition  $\times$  stress interaction:  $F_{(1,71)} = 0.26, ns$ ).

Stress was confirmed using measures of weight change (Supplementary Fig 2) and adrenal weight. Adrenal-weight-to-body-weight ratios were altered by hormonal condition (males:  $F_{(3,45)} = 12.27, p < .001$ ; females:  $F_{(3,72)} = 46.87, p < .001$ ) and stress ( $F_{(1,45)} = 30.61, p < .001$ ; females:  $F_{(1,72)} = 54.13, p < .001$ ). In unstressed males, adrenal weight was comparable across SHAM, CAST, and CAST+T groups, whereas treatment with E increased this in males ( $p < .001$ , Fig 2B). Chronic stress induced adrenal hypertrophy in SHAM, CAST, and CAST+T males ( $p < .05$ ). Likewise, adrenal weight was comparable across unstressed SHAM, OVX, and OVX+E females. Treatment with DHT decreased this compared to all other unstressed female groups ( $p < .001$ ). Stress induced adrenal hypertrophy in female rats ( $p < .01$ ; Fig 2B). Stress effects on adrenal weight did not vary with hormone manipulation in either males ( $F_{(3,45)} = 2.34, ns$ ) or females ( $F_{(3,72)} = 0.33, ns$ ).

### Basal Sex Differences in Microglia, Astrocytes, and FosB Cell Density

Microglial density differed by layer ( $F_{(2,22)} = 5.35, p < .05$ ); this did not vary with sex ( $F_{(2,22)} = 2.02, ns$ ). Microglial density was greater in unstressed SHAM females compared to SHAM males ( $F_{(1,11)} = 8.86, p < .05$ ; Fig 3A); this included all layers ( $p < .05$ ). The area of Iba-1+ material differed by layer ( $F_{(2,22)} = 6.40, p < .01$ ), and this varied between males and females ( $F_{(3,33)} = 4.54, p < .05$ ). However, the overall area of Iba-1+ material was largely comparable in unstressed animals, with only a tendency toward heightened Iba-1+ material in layer 5/6 in unstressed males ( $p = .07$ ; Fig 3B). Skeleton analyses revealed layer-specific variations in microglial process complexity ( $F_{(2,24)} = 21.71, p < .001$ ; layer  $\times$  sex:  $F_{(2,24)} = 0.34, ns$ ; Fig 3C), yet no difference between unstressed males and females ( $F_{(1,12)} = 0.31, ns$ ).

The number of astrocytes counted per image differed by layer ( $F_{(2,24)} = 10.70, p < .001$ ), but not sex ( $F$ 's  $< 0.95, ns$ ; Fig 3D). However, astrocyte morphology differed between sexes. The area of GFAP+ material differed by layer ( $F_{(2,22)} = 27.66, p < .001$ ; layer  $\times$  sex:  $F_{(2,22)} = 1.53, ns$ ), and was significantly greater in males compared to females ( $F_{(1,11)} = 10.82, p < .01$ ; Fig 3E); this included layers 2/3 ( $p = .05$ ) and 5/6 ( $p < .01$ ). Skeleton analyses revealed a tendency toward layer-specific, sex-dependent variations in astrocyte process complexity (layer:  $F_{(2,22)} = 10.54, p < .01$ ; layer  $\times$  sex:  $F_{(2,22)} = 2.54, p = .10$ ). Astrocytic complexity was greater in unstressed females in layer 5/6 ( $p < .05$ , Fig 3F).

FosB immunopositive cell density did not differ by layer ( $F$ 's < 2.12, ns; Supplementary Fig 3A-B). There were no differences in FosB immunopositive cell density in unstressed males and females ( $F_{(1,11)} = 3.24$ , ns).

## Experiment 1: Effects of Gonadal Hormones and Stress on Glia and Neuronal Activity in Males

**Microglial Density and Morphology**—Microglial density differed by layer ( $F_{(2,80)} = 7.25$ ,  $p < .001$ ); this did not vary with hormonal condition or stress ( $F$ 's < 1.14, ns; Fig 4A). Microglial density was not sensitive to hormone manipulation or stress ( $F$ 's < 1.20, ns).

Overall, the area of Iba-1+ material differed with hormone manipulation ( $F_{(3,45)} = 19.63$ ,  $p < .001$ ) but not stress ( $F$ 's < 0.80). The area of Iba-1+ material differed by layer ( $F_{(2, 90)} = 18.34$ ,  $p < .001$ ), and the effect of hormonal condition varied with layer ( $F_{(6,90)} = 37.13$ ,  $p < .001$ ) and stress ( $F_{(2,90)} = 3.62$ ,  $p < .05$ ; layer  $\times$  hormonal condition  $\times$  stress:  $F_{(6, 90)} = 0.66$ , ns; Fig 4B). Post-hoc comparisons detected heightened Iba-1+ material in unstressed CAST compared to SHAM males (1:  $p = .05$ , 2/3:  $p = .07$ , 5/6:  $p < .05$ ), and decreased Iba-1+ material in unstressed CAST+E males (2/3:  $p < .01$ , 5/6:  $p < .01$ ). In fact, Iba-1+ material was significantly reduced in CAST+E animals compared to all other unstressed groups (2/3:  $p < 0.001$ , 5/6:  $p < 0.01$ ).

Microglial process complexity differed by hormonal condition ( $F_{(3,44)} = 8.27$ ,  $p < .001$ ), but not stress ( $F$ 's < 1.90, ns). Moreover, process complexity differed by layer ( $F_{(2,88)} = 162.04$ ,  $p < .001$ ); this varied with hormonal condition ( $F_{(6,88)} = 13.59$ ,  $p < .001$ ) and stress ( $F_{(2,88)} = 3.52$ ,  $p < .05$ ; layer  $\times$  hormonal condition  $\times$  stress:  $F_{(6,88)} = 0.29$ , ns; Fig 4C). There was a tendency toward increased microglial process complexity in unstressed CAST males compared to SHAM animals (2/3:  $p = .10$ ; 5/6:  $p = .07$ ); this increase was significant compared to CAST+T (1:  $p < .05$ , 2/3:  $p < .01$ , 5/6:  $p < .01$ ) and CAST+E (layers 2/3 and 5/6:  $p < .001$ ) males. Microglial complexity was decreased in unstressed CAST+E compared to SHAM animals (2/3:  $p < .01$ , 5/6:  $p < .05$ ). Stress-induced a tendency toward decreased microglial complexity in CAST (2/3:  $p = .07$ ) and increased complexity in CAST+T (1:  $p = .05$ , 5/6:  $p = .09$ ) animals.

Microglial density, the area of Iba-1+ material, and process complexity were not strongly correlated in SHAM, CAST+T, or CAST+E treated males—this was largely true of all layers. In contrast, microglial density and area were highly correlated in CAST males (1:  $r_{(12)} = 0.72$ ,  $p < .01$ , 2/3:  $r_{(12)} = 0.66$ ,  $p < .05$ ).

**Astrocyte Counts and Morphology**—Neither hormonal condition nor stress affected the number of astrocytes counted per image ( $F$ 's < 2.58, ns; Fig 5A). However, astrocyte counts differed by layer ( $F_{(2,80)} = 8.80$ ,  $p < .001$ ), and this varied with hormonal condition ( $F_{(6,80)} = 2.85$ ,  $p < .05$ ) but not stress ( $F$ 's < 0.64, ns). Post hoc analyses indicate decreased astrocyte counts in CAST and CAST+T males compared to SHAM animals (1:  $p < .05$ ).

There were no effects of hormonal condition or stress on the area of GFAP+ material in PL ( $F$ 's < 1.04, ns); however, analyses revealed hormone-dependent stress effects on GFAP+ area ( $F_{(3,42)} = 4.75$ ,  $p < .01$ ). GFAP+ area differed by layer ( $F_{(2,84)} = 63.03$ ,  $p < .001$ );



neither hormonal condition nor stress affected this ( $F$ 's < 1.37, ns; Fig 5B). There was a tendency toward reduced GFAP+ material in CAST+E males (2/3:  $p = .06$ ). Chronic stress reduced the area of GFAP+ material in SHAM males (2/3:  $p < .01$ , 5/6:  $p < .05$ ). In contrast, stress increased GFAP+ area in CAST+E males (layers 2/3 and 5/6:  $p < .05$ ). Additional analyses indicate a tendency toward stress-induced reductions in GFAP+ area specific to layer 1 in CAST males ( $p = .07$ ).

We also analyzed astrocyte process complexity in PL. Astrocyte complexity did not differ by hormonal condition ( $F_{(3,40)} = 1.11$ , ns). However, stress affected process complexity ( $F_{(1, 40)} = 7.32$ ,  $p < .01$ ; hormonal condition  $\times$  stress interaction:  $F_{(3,40)} = 0.20$ , ns). Layer specific differences in astrocytic complexity ( $F_{(2,80)} = 14.49$ ,  $p < .001$ ) varied with hormone manipulation ( $F_{(6,80)} = 2.79$ ,  $p < .05$ ) but not stress ( $F$ 's < 0.76, ns; Fig 5C). Astrocytic complexity was reduced in CAST+T compared to SHAM males (2/3:  $p < .05$ ). There was a tendency toward a stress-induced increase in process complexity in SHAM (5/6:  $p = .06$ ), CAST+T (2/3:  $p < .05$ ), and CAST+E males (2/3:  $p < .05$ , 5/6:  $p = .09$ ).

The number of astrocytes counted was not significantly correlated with astrocyte area in males, regardless of group. However, astrocyte counts varied inversely with process complexity in SHAM (1:  $r_{(12)} = -0.63$ ,  $p < .05$ ) and CAST+T (1:  $r_{(11)} = -0.61$ ,  $p < .05$ ) animals. Astrocyte area was significantly correlated with process complexity in CAST (2/3:  $r_{(12)} = 0.82$ ,  $p < 0.01$ ), CAST+T (5/6:  $r_{(11)} = 0.61$ ,  $p < 0.01$ ), and CAST+E (2/3:  $r_{(13)} = 0.72$ ,  $p < 0.01$ , 5/6:  $r_{(13)} = 0.61$ ,  $p < 0.05$ ) males.

**FosB Immunopositive Cell Density—** FosB immunopositive cell density differed with hormone manipulation ( $F_{(3, 39)} = 4.07$ ,  $p < .05$ ), and this varied with stress ( $F_{(1, 39)} = 3.82$ ,  $p < .05$ ; stress:  $F_{(3, 39)} = 0.01$ , ns). Immunopositive cell density differed by layer ( $F_{(1, 39)} = 38.06$ ,  $p < .001$ ), and this varied with hormone manipulation ( $F_{(3, 39)} = 4.21$ ,  $p < .05$ ) but not stress ( $F < 0.03$ , ns). Stress increased FosB in layers 2/3 and 5/6 in CAST+E males ( $p < .01$ ; Supplementary Fig 3A).

**Correlations Among Glial Density, Morphology, and Neuronal Activation—** Neuron-glia and glia-glia associations in mPFC were examined in male rats (Fig 6A). FosB density was largely uncorrelated with microglial measures. However, FosB immunopositive cell density in layer 5/6 was associated with astrocyte area in apical dendritic arbor-rich laminae in males, regardless of hormone manipulation (Fig 6B). CAST males exhibited a slightly different pattern: FosB density in layer 5/6 was negatively correlated with astrocyte counts.

Microglial and astrocyte measures were only sparsely correlated in SHAM males (Fig 6C). However, in CAST males, astrocyte counts correlated with microglial density and area. The pattern of associations between glial measures were similar in SHAM and CAST+T animals; however, these correlations were stronger in CAST+T males. In contrast, microglial density and astrocyte counts were inversely related in CAST+E males.

Stress induced a strong, negative relationship between FosB density and microglial measures, but had few effects on the positive association between FosB density and

astrocyte morphology (Fig 6D). Stress altered various correlations between microglia and astrocytes, producing negative associations across measures of microglial and astrocyte morphology (Fig 6E).

## Experiment 2: Effects of Gonadal Hormones and Stress on Glia and Neuronal Activity in Females

**Microglial Density and Morphology**—In females, microglial density differed with hormonal condition ( $F_{(3,52)} = 3.17, p < .05$ ), and stress effects on microglial density varied with hormone manipulation ( $F_{(3,52)} = 3.05, p < .05$ ; effect of stress:  $F_{(1,52)} = 0.15, ns$ ). Microglial density differed by layer ( $F_{(2,104)} = 10.22, p < .001$ ). This did not vary with hormone manipulation or stress ( $F$ 's  $< 1.76, ns$ ; Fig 7A). Microglial density was decreased in unstressed OVX+DHT compared to unstressed SHAM (1:  $p = .05, 2/3: p < .01, 5/6: p < .05$ ), OVX (1:  $p < .01, 2/3: p < .05, 5/6: p = 0.08$ ), and OVX+E (1 and 2/3:  $p < .01$ ) females. Chronic stress decreased microglial density in SHAM (2/3:  $p < .05, 5/6: p = .07$ ), yet increased microglia density in OVX+DHT females (1:  $p < .05$ ).

The area of Iba-1+ material differed with hormone manipulation ( $F_{(3,50)} = 4.08, p < .05$ ) and stress ( $F_{(1,50)} = 8.19, p < .01$ ). Stress effects on Iba-1+ area varied with hormone treatment ( $F_{(3,50)} = 6.18, p < .001$ ). Moreover, Iba-1+ area was layer-specific in females ( $F_{(2,100)} = 154.08, p < .001$ ), and this varied with both hormonal condition ( $F_{(6,100)} = 85.23, p < .001$ ) and stress ( $F_{(2,100)} = 8.34, p < .001$ ; layer  $\times$  hormonal condition  $\times$  stress:  $F_{(6,100)} = 5.57, p < .001$ ; Fig 7B). Post hoc analyses indicate reduced Iba-1+ area in layers 2/3 and 5/6 ( $p < .01$ ) in unstressed OVX+DHT females compared to all other unstressed groups. Chronic stress reduced the area of Iba-1+ material in SHAM and OVX+E females (all layers:  $p < .05$ ). There were no effects of stress on Iba-1+ area in OVX females. In contrast, stress increased Iba-1+ area in OVX+DHT females (1:  $p < .001$ ).

Microglial process complexity did not differ by hormonal condition ( $F_{(3,55)} = 0.94, ns$ ). However, stress effects on microglial complexity ( $F_{(1,55)} = 4.52, p < .05$ ) were hormone dependent ( $F_{(3,55)} = 2.97, p < .05$ ). Process complexity differed by layer in females ( $F_{(2,110)} = 71.73, p < .001$ ); this did not vary with hormonal condition or stress ( $F$ 's  $< 1.67, ns$ ; Fig 7C). Microglial complexity was reduced in unstressed OVX+DHT compared to unstressed SHAM, OVX, and OVX+E females (2/3:  $p < .05$ ). Chronic stress reduced process complexity in SHAM (1:  $p < .05, 2/3: p = .11, 5/6: p = .11$ ) and OVX+E (1:  $p < .05, 2/3: p = .07, 5/6: p < .01$ ) animals. In contrast, there was a stress-induced tendency toward increased microglial complexity in OVX+DHT females (2/3:  $p = .09$ ).

Correlations between microglial density and morphology were also examined. Microglial density was not significantly correlated with the area of Iba-1+ material or microglial complexity in female rats – this was true of most layers. However, Iba-1+ area was significantly correlated with microglial complexity in SHAM (1:  $r_{(15)} = 0.57, p < .05, 2/3: r_{(16)} = 0.56, p < .05, 5/6: r_{(16)} = 0.78, p < .01$ ) and OVX+E females (1:  $r_{(15)} = 0.87, p < .001, 2/3: r_{(15)} = 0.68, p < .01, 5/6: r_{(15)} = 0.61, p < .05$ ).

**Astrocyte Counts and Morphology**—The number of astrocytes counted per image was affected by hormone manipulation ( $F_{(3,54)} = 6.10, p < .01$ ), but not stress ( $F$ 's  $< 1.58, ns$ ).

Astrocyte counts differed by layer ( $F_{(2,108)} = 28.39$ ,  $p < .001$ ), and this did not vary with hormonal condition or stress ( $F$ 's  $< 1.35$ , ns; Fig 8A). Post hoc analyses indicate a slight reduction in astrocyte counts in OVX+E females (1:  $p < .05$ ), and a tendency toward greater astrocyte numbers in OVX+DHT animals (1:  $p = .08$ ).

The area of GFAP+ material was sensitive to hormone manipulation ( $F_{(3,52)} = 10.40$ ,  $p < .001$ ) and stress ( $F_{(1,52)} = 6.88$ ,  $p < .01$ ; hormonal condition  $\times$  stress interaction:  $F_{(3,52)} = 0.67$ , ns). Astrocyte morphology also differed by layer ( $F_{(2,104)} = 162.51$ ,  $p < .001$ ); this did not vary with hormonal condition or stress ( $F$ 's  $< 1.36$ , ns; Fig 8B). Astrocyte area was increased in unstressed OVX+DHT females compared to all other unstressed groups (1:  $p < .05$ , 2/3:  $p < .01$ , 5/6:  $p < .05$ ). Chronic stress increased GFAP+ area in SHAM females (2/3:  $p < .05$ , 5/6:  $p < .01$ ).

Astrocyte process complexity was unaffected by hormone manipulation or stress ( $F$ 's  $< 0.73$ , ns). However, analyses revealed layer-specific differences in astrocyte complexity ( $F_{(2,110)} = 38.27$ ,  $p < .001$ ). These differences did not vary with hormonal condition or stress ( $F$ 's  $< 2.02$ , ns; Fig 8C). Post hoc comparisons indicate greater process complexity in layer 1 ( $p < .05$ ) and reduced process complexity in layer 5/6 ( $p = .08$ ) in unstressed OVX+E compared to SHAM animals. Stress reduced astrocyte complexity in SHAM females (5/6:  $p < .05$ ).

The number of astrocytes was not significantly correlated with GFAP+ area in most layers, regardless of hormonal manipulation. However, similar to males, astrocyte numbers were inversely related to process complexity in SHAM (5/6:  $r_{(16)} = -0.92$ ,  $p < .001$ ), OVX (5/6:  $r_{(15)} = -0.79$ ,  $p < .001$ ), OVX+E (5/6:  $r_{(16)} = -0.66$ ,  $p < .01$ ), and OVX+DHT (2/3:  $r_{(15)} = -0.84$ ,  $p < .001$ , 5/6:  $r_{(15)} = -0.61$ ,  $p < .05$ ) animals. Astrocyte area and complexity were correlated in OVX females only (2/3:  $r_{(15)} = 0.66$ ,  $p < .01$ ).

**FosB Immunopositive Cell Density—** FosB immunopositive cell density was not altered by hormone manipulation ( $F_{(3,51)} = 2.58$ , ns) or stress ( $F_{(1,51)} = 3.54$ ,  $p < .05$ ; hormonal condition  $\times$  stress interaction:  $F_{(3,51)} = 0.21$ , ns) in females (Supplementary Fig 3B). However, FosB cell density differed by layer ( $F_{(1,51)} = 27.71$ ,  $p < .001$ ); this did not vary with hormonal condition or stress ( $F$ 's  $< 1.95$ , ns).

**Correlations Among Glial Density, Morphology, and Neuronal Activation—** Neuron-glia and glia-glia associations in mPFC were examined in female rats (Fig 9A).

FosB immunopositive cell density in layer 2/3 was negatively correlated with microglial density in SHAM females only (Fig 9B). FosB density in either layer 2/3 or 5/6 associated with astrocyte counts and morphology, regardless of hormone manipulation. In contrast to all other female groups, FosB density in layer 5/6 associated with microglial density and area, but not astrocyte counts or morphology, in OVX+DHT females.

Hormonal manipulation produced a distinct pattern of microglia-astrocyte association in each respective group (Fig 9C). Microglial complexity was negatively correlated with astrocyte measures in SHAM females. Astrocyte counts were correlated with microglial area, and astrocyte area associated with microglial area in OVX+E animals. Relatively few significant correlations were detected in OVX and OVX+DHT females.

FosB cell density and microglial density and morphology were largely negatively correlated in unstressed females; chronic stress either reduced or reversed this pattern (Fig 9D). FosB density in both layers 2/3 and 5/6 associated with astrocyte number and morphology, and stress disrupted this. Generally, microglial and astrocyte measures were negatively correlated in unstressed females and this was – similar to microglia-neuron associations – reversed by stress (Fig 9E).

## Discussion

Here we report basal sex differences in microglia and astrocytes in mPFC, alongside sex-specific patterns of chronic stress-induced glial remodeling. These sex-specific stress effects on glial morphology in mPFC were gonadal hormone-dependent (Fig 10).

### Increased Microglial Density in mPFC in Females, Greater Astrocyte Area in Males

Microglial density was greater in mPFC in unstressed females compared to males. A non-significant tendency toward this can be seen in Bollinger, Burns (11). However, unlike previous reports, the area of Iba-1+ material (i.e. microglial coverage) and measures of microglial process complexity were similar between males and females. This discrepancy may be due to differences in technique. Prior studies assessed microglia using morphological classification, whereas this study assessed components of microglial morphology. Taken together, these data complement reports of increased microglial density and activation in other brain regions in females (49). Heightened microglial density might indicate increased surveillance in mPFC in females. Moreover, microglial morphological characteristics associated with greater activity suggest the potential for heightened monitoring or dendritic sculpting (50). Given such, it is interesting to speculate that sex differences in microglia in mPFC might contribute to sex differences in neuronal complexity and function. For instance, heightened microglial monitoring could contribute to increased dendritic sculpting and, in turn, reduced apical dendritic arbor length in mPFC in females compared to males.

We also found pronounced sex differences in astrocyte morphology in mPFC. The area of GFAP+ material and astrocyte process complexity was greater in males compared to females. This suggests increased process thickness in males. GFAP is typically expressed in primary processes, from which synapse-associated secondary branches radiate (51). Astrocytes play a critical role in maintaining synaptic structure and plasticity (26). Thus, increased primary process thickness might allow for increased secondary branching and greater synaptic support. Again, this is consistent with sex differences in neuronal architecture in mPFC: males have larger apical dendritic arbors (9, 52), possibly necessitating heightened astrocyte support (53). However, not all astrocytic processes express GFAP (i.e. most secondary processes do not); therefore, sex differences in astrocyte morphology may be more complex than reported here. Future studies examining sex differences in astrocyte dynamics and secondary structure are warranted.

### **Gonadal Hormones Regulate Microglial Morphology in mPFC in Males**

Gonadectomy increased microglial complexity and area in mPFC in males, without any change in cell density. This effect was observed – largely – across all layers of mPFC, and may indicate “priming” or heightened activity absent of proliferation or migration. Supplementation with T prevents this, indicating that T regulates basal microglial state. As T can be locally metabolized into E, its effects may be driven by either AR- or ER-mediated actions, or a combination of receptor pathways. In line with this, administration of E reduced microglial morphological activation in males beyond that produced by T. Other studies indicate reduced microglial activation in a penetrating brain injury model following administration of T, its metabolites E or DHT (54), or selective ER modulators (55). Notably, DHT is only effective in reducing microglial activation if administered early post-injury, whereas T and E are effective regardless of administration time (54). These data indicate that either AR or ER-mediated actions can modulate microglial morphology in males.

In females, basal microglial and astrocyte morphology was not affected by OVX. However, administration of DHT increased basal astrocyte counts and area to male-typical levels. Estrogens and androgens maintain dendritic architecture and – potentially – mediate dendritic growth in corticolimbic circuitry. For instance, treatment with T or E prevents OVX-induced dendritic spine atrophy in hippocampus in females (56), whereas T – but not E – inhibits the effects of castration on dendritic spines in males (57). If androgens stimulate dendritic growth in females, masculinized dendritic complexity might necessitate heightened astrocyte support and, in turn, increased astrocyte area (53). Conversely, androgenic actions on astrocytes might drive dendritic growth, as astrocytic factors can regulate dendritic branching (58) and spine maturation (59).

### **Chronic Stress Effects on Microglia in mPFC are Dependent on Gonadal Hormones in Females, not Males**

Chronic restraint stress reduces microglial morphology and immune factor expression in mPFC in females (11). Likewise, chronic stress reduced microglial area in mPFC in SHAM females. Given that microglial density and area were not significantly correlated, decreased number of microglia is likely not responsible for this finding. Rather, stress-induced reductions in microglial area in mPFC appear to reflect microglial remodeling, including process retraction, reductions in overall process length, and decreased cell thickness. Microglial processes interact with neuronal elements, and are capable of shaping synapses (15, 60). Thus, fewer microglial processes may result in reduced ‘synaptic scanning’ and – in turn – allow for dendritic reorganization or growth (50). Consistent with this, similar chronic stress paradigms either induce no change in neuronal architecture in mPFC (8), or increase apical dendritic arbor complexity (9) and dendritic spine density (10) in females. These stress-induced increases in dendritic complexity may underlie alterations in prefrontal function and behavior.

Microglia express ER’s (22), and E can shape microglial morphology and function (15). Moreover, E modulates stress effects on neuronal morphology in mPFC (9) and mPFC-mediated behavior (39), suggesting a role for this hormone in stress-linked microglial

atrophy in females. Indeed, in this study, OVX blocked stress effects on microglial morphology in mPFC, whereas E replacement restored them. Thus, E is necessary for remodeling of microglial morphology in females. These findings are congruent with reports indicating a protective role for E in endotoxin-induced microglial activation (16), and align with potential microglial involvement in stress-linked dendritic remodeling: OVX prevents stress effects on dendritic complexity in mPFC in females, whereas estradiol replacement is permissive of stress-induced dendritic growth (9).

Interestingly, stress produced microglial morphological remodeling consistent with heightened activity in mPFC in DHT-treated females. This is similar to stress effects in male rats, wherein acute (11) and chronic stress (20, 21) induce microglial hypertrophy and ramification in mPFC. AR's are not readily detectable in surveillant microglia; however, microglia can express AR's following a severe perturbation (e.g. stab wound injury; 23). It is unclear whether psychological stress induces expression of microglial AR's. Given that microglia only selectively express these receptors, the effects of DHT on microglia may be indirect and, in turn, mediated by cell-to-cell interaction or signals associated with the neural milieu. This remains unexplored.

As previously reported, chronic stress did not affect microglial morphology in mPFC in males (11). A number of factors likely contribute to this finding, including stressor severity, duration, predictability, and the temporal pattern of stress-induced microglial remodeling. Stress effects were not unmasked with hormone manipulation. Therefore, stress effects on microglial morphology in males are likely independent of gonadal hormones, and may be attuned to fluctuations within the local, neuronal – rather than endocrine – environment. However, further studies are needed examining the role of gonadal hormones in stress models that induce significant microglial remodeling in males (i.e. social defeat stress, longer/more severe restraint paradigms; 21, 61).

### **Sex-Specific Patterns of Stress-Induced Astrocyte Remodeling in mPFC are Modulated by Gonadal Hormones**

Numerous studies report stress-linked reductions in astrocytic material and function in mPFC in males (28, 31). Likewise, we found restraint stress-induced reductions in astrocyte area in mPFC in SHAM males. As astrocytic processes support dendritic spines and shape synaptic function (26), this finding correlates well with stress-induced reductions in dendritic spine density (62) and dendritic atrophy (44) in males. However, in females, stress-induced increases in dendritic branching and length in mPFC (9) may require heightened astrocyte support (53). Indeed, chronic stress increased astrocyte area and complexity in mPFC in SHAM females, suggesting process enlargement, perhaps in support of dendritic growth.

In males, gonadectomy with or without T replacement prevented the effects of stress on astrocyte area, whereas administration of E allowed for a stress-induced increase in astrocytic material. As gonadectomy blocked the effects of stress, circulating gonadal hormones likely contribute to stress-induced astrocyte atrophy. However, administration of T did not restore stress effects on astrocyte morphology. One potential explanation may be related to differences in T – and in turn – E availability. T levels in gonadectomized rats with

silastic implants remain stable, and are consistently higher than that of control rats (63). Moreover, animals with T implants have considerably higher levels of circulating E (63). In this study, administration of E allowed for a stress-induced increase in astrocyte area. If stable, consistently available levels of T are more readily converted to E, competing actions of androgens (atrophy) and estrogens (hypertrophy) might mask stress effects on astrocyte morphology. This hypothesis is consistent with trends in the data, wherein there is a non-significant tendency toward reduced astrocyte area in unstressed males treated with either T or E.

Gonadectomy prevents stress-linked dendritic remodeling in mPFC in females (9, 10), and in this study reduced stress effects on astrocyte morphology. Supplementation with E restores stress-induced dendritic growth – but not branching – in mPFC (9). Likewise, E replacement leads to a different pattern of astrocyte remodeling: a tendency toward increased astrocyte area regardless of stress, and stress-induced astrocyte process extension. On the other hand, OVX blocked stress effects on all assessed measures of astrocyte morphology. Thus, gonadal hormones appear to play a role in regulating stress-linked shifts in astrocytes, though the specifics of this remain elusive. Stress effects on astrocyte morphology may be sensitive to estrous cycle-dependent fluctuations. Indeed, astrocyte morphology varies over the estrous cycle (64), and modulation of this pattern (i.e. OVX or OVX+E) may have unexpected consequences for astrocyte responsivity. Our data support this notion. Administration of DHT increased astrocyte area in mPFC, effectively masculinizing the morphological profile of astrocytes. This overall increase may have masked potential stress effects on astrocyte morphology.

### **Chronic Restraint Stress Does Not Induce Significant FosB Expression in mPFC**

Hormonal manipulation or stress did not broadly influence the density of FosB immunopositive cells in mPFC in male or female rats. Several reports indicate chronic immobilization- (1 h/day, 10 days; 40) or restraint- associated (6 h/day, 21 days; 21) FosB induction in mPFC in males, whereas others find no change in FosB expression following chronic restraint- (1 h/day, 14 days; 65), noise- (30 min/day, 12 days; 66) or social defeat-stress (10 min/day, 10 days; 67). Taken together, these studies suggest severity- and duration-dependent effects of stress on FosB induction. Therefore, it is not surprising that the chronic restraint paradigm used in this study failed to evoke FosB expression. In fact, this is consistent with data linking longer-duration, more intense (6 h/day) restraint stress-associated FosB induction with microglial hypertrophy in mPFC (21). The shorter-term, less intense chronic stress used in this study had no effect on microglial morphology in males.

Accumulation of FosB is linked with repeated neuronal activation (67). Thus, these data suggest similar levels of repeated neuronal activity in mPFC in males and females, regardless of hormonal condition or stress. This suggests that hormonal effects on microglial morphology were not mediated by hormonal modulation of neuronal activity. Instead, our data indicate that direct hormone-microglia actions or indirect signaling through other glia or non-neuronal cells may mediate these effects. Moreover, these findings, in conjunction

with stress effects on adrenal weight suggest that hormonal manipulation does not alter the severity or overall experience of chronic restraint stress.

### **Layer 5/6 Neuronal Activity is Associated with Astrocyte Number and Morphology in mPFC in Both Sexes; Stress Enhances Neuron-Microglia Coupling in Males, Reduces Neuron-Astrocyte Coupling in Females**

FosB expression in layer 5/6 was highly correlated with measures of astrocyte number and morphology across mPFC laminae in male and female rats, regardless of hormone manipulation. Neuronal activity can regulate astrocyte morphology, gene expression, and maturation (68). Thus, these data suggest that neuronal activity in layer 5/6 in mPFC may influence astrocyte morphology in more superficial, apical dendritic arbor-rich layers (layers 1, 2/3). Conversely, astrocytes can support synaptic maintenance through resource exchange and trophic factor expression, and regulate synaptic transmission via neurotransmitter uptake (25). Therefore, astrocytic support on apical dendritic arbors may facilitate neurotransmission and, in turn, be coupled with layer 5/6 excitation. The functional role of this coupling has yet to be elucidated. However, it is interesting to speculate that this glia-neuron connection in mPFC may be involved in maintaining neuronal function in layer 5/6, and might play a role in attenuating stress effects on apical dendritic complexity in large, layer 5/6 neurons.

Collapsed across hormonal groups, stress induced a negative association between neuronal activity and microglial morphology in males, yet had a stronger effect on neuronal activity-astrocyte coupling in females. Although stress had little effect on FosB expression in either sex, it is possible that subtle, stress-induced shifts in neuronal activity contribute to microglial changes in males, and astrocyte alterations in females. The converse is equally plausible. Together, these data suggest that neuronal activity-glia interactions are not ubiquitous across glial cell type, and that sex-specific pathways may direct neuronal activity-glia coupling.

### **Other Hormonal Pathways**

We focused on androgens and estrogens in this study. However, progestins may also modulate glial morphology and function in mPFC. Stress increases the level of progesterone (P) in frontal cortex in both males and females (69), and neurons, astrocytes, and microglia can all express P receptors (PR's; 70). Furthermore, gonadal steroids interact with other stress-associated hormones, including glucocorticoids (71). Although stressed animals show pronounced weight loss and adrenal hypertrophy regardless of hormonal manipulation, modulating gonadal hormones may have altered glucocorticoid availability, receptor expression, and/or subsequent glucocorticoid-brain signaling cascades.

These data indicate sex differences in microglial density and astrocyte morphology in mPFC, alongside hormone-dependent stress effects on glia in males and females. Such findings parallel sex differences in prefrontal neuronal structure, and are congruent with reports of sex- and hormone-dependent stress effects on neuronal architecture and function in mPFC. Thus, glia may play a critical role in regulating sex differences in stress effects on neuronal plasticity and behavior. Indeed, these preclinical findings are in line with post-



mortem data that indicate divergent neuronal and microglial gene expression profiles in frontal cortex in males and females with depression: men show reduced neuronal and heightened microglial transcripts, whereas women show the opposite (72). Our findings provide insight into potential contributions of gonadal hormones to these unique neuronal and glial signatures in depression. Moreover, our findings call for future experiments examining the sex-dependent neural and behavioral ramifications of microglial remodeling, astrocyte restructuring, and glia-neuron interaction in stress.

## Supplementary Material

Refer to Web version on PubMed Central for supplementary material.

## Acknowledgement of Funding Sources:

This work was supported by Indiana University, the National Institute of Mental Health (T32MH103213 to JLB), and the National Institute of Child Health and Human Development (T32HD049336 to JLB).

## References

1. Maciejewski PK, Prigerson HG, Mazure CM. Sex differences in event-related risk for major depression. *Psychol Med* 2001;31(4):593–604. [PubMed: 11352362]
2. Kessler RC, Berglund P, Demler O, Jin R, Walters EE. Lifetime prevalence and age-of-onset distributions' of DSM-IV disorders in the national comorbidity survey replication. *Arch Gen Psychiatry* 2005;62(6):593–602. [PubMed: 15939837]
3. Bebbington P The origins of sex differences in depressive disorder: Bridging the gap. *Int Rev Psych* 1996;8(4):295–332.
4. Marcus SM, Young EA, Kerber KB, Kornstein S, Farabaugh AH, Mitchell J, et al. Gender differences in depression: Findings from the STAR\*D study. *J Affect Disord* 2005;87(2–3):141–50. [PubMed: 15982748]
5. Breslau J, Gilman SE, Stein BD, Ruder T, Gmelin T, Miller E. Sex differences in recent first-onset depression in an epidemiological sample of adolescents. *Transl Psychiatry* 2017;7:e1139. [PubMed: 28556831]
6. McIntyre RS, Mancini D, Eisfeld BS, Soczynska JK, Grupp L, Konarski JZ, et al. Calculated bioavailable testosterone levels and depression in middle-aged men. *Psychoneuroendocrinology* 2006;31(9):1029–35. [PubMed: 16908107]
7. Seidman SN, Araujo AB, Roose SP, McKinlay JB. Testosterone level, androgen receptor polymorphism, and depressive symptoms in middle-aged men. *Biological Psychiatry* 2001;50(5):371–6. [PubMed: 11543741]
8. Moench KM, Wellman CL. Differential dendritic remodeling in prelimbic cortex of male and female rats during recovery from chronic stress. *Neuroscience* 2017;357:145–59. [PubMed: 28596115]
9. Garrett JE, Wellman CL. Chronic stress effects on dendritic morphology in medial prefrontal cortex: Sex differences and estrogen dependence. *Neuroscience* 2009;162(1):195–207. [PubMed: 19401219]
10. Shansky RM, Hamo C, Hof PR, Lou W, McEwen BS, Morrison JH. Estrogen Promotes Stress Sensitivity in a Prefrontal Cortex-Amygdala Pathway. *Cereb Cortex* 2010;20(11):2560–7. [PubMed: 20139149]
11. Bollinger JL, Burns CMB, Wellman CL. Differential effects of stress on microglial cell activation in male and female medial prefrontal cortex. *Brain Behav Immun* 2016;52:88–97. [PubMed: 26441134]
12. Wohleb ES, Terwilliger R, Duman CH, Duman RS. Stress-induced neuronal CSF1 provokes microglia-mediated neuronal remodeling and depressive-like behavior. *Biological Psychiatry* 2017.

13. Salter MW, Beggs S. Sublime Microglia: Expanding Roles for the Guardians of the CNS. *Cell* 2014;158(1):15–24. [PubMed: 24995975]
14. Salter MW, Stevens B. Microglia emerge as central players in brain disease. *Nat Med* 2017;23:1018. [PubMed: 28886007]
15. Lenz KM, Nugent BM, Haliyur R, McCarthy MM. Microglia Are Essential to Masculinization of Brain and Behavior. *Journal of Neuroscience* 2013;33(7):2761–72. [PubMed: 23407936]
16. Ishihara Y, Itoh K, Ishida A, Yamazaki T. Selective estrogen-receptor modulators suppress microglial activation and neuronal cell death via an estrogen receptor-dependent pathway. *J Steroid Biochem Mol Biol* 2015;145:85–93. [PubMed: 25305410]
17. Nelson LH, Saulsbery AI, Lenz KM. Small cells with big implications: Microglia and sex differences in brain development, plasticity and behavioral health. *Prog Neurobiol* 2018.
18. Villa A, Gelosa P, Castiglioni L, Cimino M, Rizzi N, Pepe G, et al. Sex-Specific Features of Microglia from Adult Mice. *Cell Reports* 2018;23(12):3501–11. [PubMed: 29924994]
19. De Biase LM, Schuebel KE, Fusfeld ZH, Jair K, Hawes IA, Cimbri R, et al. Local Cues Establish and Maintain Region-Specific Phenotypes of Basal Ganglia Microglia. *Neuron* 2017;95(2):341–56.e6. [PubMed: 28689984]
20. Tynan RJ, Naicker S, Hinwood M, Nalivaiko E, Buller KM, Pow DV, et al. Chronic stress alters the density and morphology of microglia in a subset of stress-responsive brain regions. *Brain Behav Immun* 2010;24(7):1058–68. [PubMed: 20153418]
21. Hinwood M, Morandini J, Day TA, Walker FR. Evidence that Microglia Mediate the Neurobiological Effects of Chronic Psychological Stress on the Medial Prefrontal Cortex. *Cereb Cortex* 2012;22(6):1442–54. [PubMed: 21878486]
22. Sierra A, Gottfried-Blackmore A, Milner TA, McEwen BS, Bulloch K. Steroid hormone receptor expression and function in microglia. *Glia* 2008;56(6):659–74. [PubMed: 18286612]
23. Garcia-Ovejero D, Veiga S, Garcia-Segura LM, DonCarlos LL. Glial expression of estrogen and androgen receptors after rat brain injury. *Journal of Comparative Neurology* 2002;450(3):256–71. [PubMed: 12209854]
24. Bender CL, Calfa GD, Molina VA. Astrocyte plasticity induced by emotional stress: A new partner in psychiatric physiopathology? *Progress in Neuro-Psychopharmacology and Biological Psychiatry* 2016;65:68–77. [PubMed: 26320029]
25. Allen NJ, Eroglu C. Cell Biology of Astrocyte-Synapse Interactions. *Neuron* 2017;96(3):697–708. [PubMed: 29096081]
26. Chung WS, Allen NJ, Eroglu C. Astrocytes Control Synapse Formation, Function, and Elimination. *Cold Spring Harbor Perspect Biol* 2015;7(9):18.
27. Tian L, Ma L, Kaarela T, Li Z. Neuroimmune crosstalk in the central nervous system and its significance for neurological diseases. *J Neuroinflamm* 2012;9(1):155.
28. Tynan RJ, Beynon SB, Hinwood M, Johnson SJ, Nilsson M, Woods JJ, et al. Chronic stress-induced disruption of the astrocyte network is driven by structural atrophy and not loss of astrocytes. *Acta Neuropathol* 2013;126(1):75–91. [PubMed: 23512378]
29. Sun J-D, Liu Y, Yuan Y-H, Li J, Chen N-H. Gap Junction Dysfunction in the Prefrontal Cortex Induces Depressive-Like Behaviors in Rats. *Neuropsychopharmacology* 2011;37:1305. [PubMed: 22189291]
30. Banasr M, Chowdhury GMI, Terwilliger R, Newton SS, Duman RS, Behar KL, et al. Glial pathology in an animal model of depression: reversal of stress-induced cellular, metabolic and behavioral deficits by the glutamate-modulating drug riluzole. *Mol Psychiatr* 2010;15(5):501–11.
31. Banasr M, Duman RS. Glial Loss in the Prefrontal Cortex Is Sufficient to Induce Depressive-like Behaviors. *Biological Psychiatry* 2008;64(10):863–70. [PubMed: 18639237]
32. Pfau DR, Hobbs NJ, Breedlove MS, Jordan CL. Sex and laterality differences in medial amygdala neurons and astrocytes of adult mice. *Journal of Comparative Neurology* 2016;524(12):2492–502. [PubMed: 26780286]
33. Garcia-Segura LM, Suarez I, Segovia S, Tranque PA, Calés JM, Aguilera P, et al. The distribution of glial fibrillary acidic protein in the adult rat brain is influenced by the neonatal levels of sex steroids. *Brain Res* 1988;456(2):357–63. [PubMed: 3061565]

34. Azcoitia I, Sierra A, Miguel Garcia-Segura L. Localization of estrogen receptor  $\beta$ -immunoreactivity in astrocytes of the adult rat brain. *Glia* 1999;26(3):260–7. [PubMed: 10340766]
35. Johnson RT, Schneider A, DonCarlos LL, Breedlove SM, Jordan CL. Astrocytes in the Rat Medial Amygdala Are Responsive to Adult Androgens. *The Journal of comparative neurology* 2012;520(11):2531–44. [PubMed: 22581688]
36. Astiz M, Acaz-Fonseca E, Garcia-Segura LM. Sex Differences and Effects of Estrogenic Compounds on the Expression of Inflammatory Molecules by Astrocytes Exposed to the Insecticide Dimethoate. *Neurotoxicity Research* 2014;25(3):271–85. [PubMed: 23943137]
37. Santos-Galindo M, Acaz-Fonseca E, Bellini MJ, Garcia-Segura LM. Sex differences in the inflammatory response of primary astrocytes to lipopolysaccharide. *Biology of Sex Differences* 2011;2(1):7. [PubMed: 21745355]
38. Fontainhas AM, Minhua W, Liang KJ, Shan C, Mettu P, Damani M, et al. Microglial Morphology and Dynamic Behavior Is Regulated by Ionotropic Glutamatergic and GABAergic Neurotransmission. *PLoS ONE* 2011;6(1):1–14.
39. Wei J, Yuen EY, Liu W, Li X, Zhong P, Karatsoreos IN, et al. Estrogen protects against the detrimental effects of repeated stress on glutamatergic transmission and cognition. *Mol Psychiatry* 2014;19(5):588–98.
40. Perrotti LI, Hadeishi Y, Ulery PG, Barrot M, Monteggia L, Duman RS, et al. Induction of Delta FosB in reward-related brain structures after chronic stress. *Journal of Neuroscience* 2004;24(47):10594–602. [PubMed: 15564575]
41. Overpeck JG, Colson SH, Hohmann JR, Applestine MS, Reilly JF. Concentrations of circulating steroids in normal prepubertal and adult male and female humans, chimpanzees, rhesus-monkeys, rats, mice, and hamsters - literature survey. *Journal of Toxicology and Environmental Health* 1978;4(5–6):785–803. [PubMed: 104044]
42. Verhovshek T, Sengelaub DR. Androgen action at the target musculature regulates brain-derived neurotrophic factor protein in the spinal nucleus of the bulbocavernosus. *Developmental Neurobiology* 2013;73(8):587–98. [PubMed: 23512738]
43. Smith ER, Damassa DA, Davidson JM. Chapter 9 - Hormone Administration: Peripheral and Intracranial Implants1 A2 - MYERS, R.D. *Methods in Psychobiology*: Academic Press; 1977 p. 259–79.
44. Cook SC, Wellman CL. Chronic stress alters dendritic morphology in rat medial prefrontal cortex. *J Neurobiol* 2004;60(2):236–48. [PubMed: 15266654]
45. Paxinos G, Watson C. *The rat brain in stereotaxic coordinates* 4th ed. New York: Academic Press; 1998.
46. Vollmer LL, Ghosal S, McGuire JL, Ahlbrand RL, Li K-Y, Santin JM, et al. Microglial Acid Sensing Regulates Carbon Dioxide-Evoked Fear. *Biological Psychiatry* 2016;80(7):541–51. [PubMed: 27422366]
47. Ganguly P, Thompson V, Gildawie K, Brenhouse HC. Adolescent food restriction in rats alters prefrontal cortex microglia in an experience-dependent manner. *Stress* 2018:1–7.
48. Bollinger JL, Collins KE, Patel R, Wellman CL. Behavioral stress alters corticolimbic microglia in a sex- and brain region-specific manner. *PLoS One* 2017;12(12):e0187631. [PubMed: 29194444]
49. Schwarz JM, Sholar PW, Bilbo SD. Sex differences in microglial colonization of the developing rat brain. *J Neurochem* 2012;120(6):948–63. [PubMed: 22182318]
50. Rappert A, Bechmann I, Pivneva T, Mahlo J, Biber K, Nolte C, et al. CXCR3-dependent microglial recruitment is essential for dendrite loss after brain lesion. *Journal of Neuroscience* 2004;24(39):8500–9. [PubMed: 15456824]
51. Middeldorp J, Hol EM. GFAP in health and disease. *Prog Neurobiol* 2011;93(3):421–43. [PubMed: 21219963]
52. Markham JA, Juraska JM. Aging and sex influence the anatomy of the rat anterior cingulate cortex. *Neurobiol Aging* 2002;23(4):579–88. [PubMed: 12009507]
53. Haber M, Zhou L, Murai KK. Cooperative Astrocyte and Dendritic Spine Dynamics at Hippocampal Excitatory Synapses. *The Journal of Neuroscience* 2006;26(35):8881–91. [PubMed: 16943543]

54. Barreto G, Veiga S, Azcoitia I, Garcia-Segura LM, Garcia-Ovejero D. Testosterone decreases reactive astroglia and reactive microglia after brain injury in male rats: role of its metabolites, oestradiol and dihydrotestosterone. *Eur J Neurosci* 2007;25(10):3039–46. [PubMed: 17561817]
55. Barreto GE, Santos-Galindo M, Garcia-Segura LM. Selective estrogen receptor modulators regulate reactive microglia after penetrating brain injury. *Front Aging Neurosci* 2014;6:7. [PubMed: 24478700]
56. Leranth C, Hajszan T, MacLusky NJ. Androgens Increase Spine Synapse Density in the CA1 Hippocampal Subfield of Ovariectomized Female Rats. *The Journal of Neuroscience* 2004;24(2):495–9. [PubMed: 14724248]
57. Leranth C, Petnehazy O, MacLusky NJ. Gonadal Hormones Affect Spine Synaptic Density in the CA1 Hippocampal Subfield of Male Rats. *The Journal of Neuroscience* 2003;23(5):1588–92. [PubMed: 12629162]
58. Zhu Y-B, Gao W, Zhang Y, Jia F, Zhang H-L, Liu Y-Z, et al. Astrocyte-derived phosphatidic acid promotes dendritic branching. *Scientific Reports* 2016;6:21096. [PubMed: 26883475]
59. Nishida H, Okabe S. Direct Astrocytic Contacts Regulate Local Maturation of Dendritic Spines. *The Journal of Neuroscience* 2007;27(2):331–40. [PubMed: 17215394]
60. Tremblay ME, Lowery RL, Majewska AK. Microglial Interactions with Synapses Are Modulated by Visual Experience. *PLoS Biol* 2010;8(11):16.
61. Lehmann ML, Cooper HA, Maric D, Herkenham M. Social defeat induces depressive-like states and microglial activation without involvement of peripheral macrophages. *J Neuroinflamm* 2016;13:19.
62. Radley JJ, Rocher AB, Miller M, Janssen WGM, Liston C, Hof PR, et al. Repeated stress induces dendritic spine loss in the rat medial prefrontal cortex. *Cereb Cortex* 2006;16(3):313–20. [PubMed: 15901656]
63. Dykman DD, Cochran R, Wise PM, Barraclough CA, Dubin NH, Ewing LL. Temporal Effects of Testosterone-Estradiol Polydimethylsiloxane Subdermal Implants on Pituitary, Leydig Cell, and Germinal Epithelium Function and Daily Serum Testosterone Rhythm in Male Rats I. *Biol Reprod* 1981;25(2):235–43. [PubMed: 7197991]
64. Arias C, Zepeda A, Hernandez-Ortega K, Leal-Galicia P, Lojero C, Camacho-Arroyo I. Sex and estrous cycle-dependent differences in glial fibrillary acidic protein immunoreactivity in the adult rat hippocampus. *Horm Behav* 2009;55(1):257–63. [PubMed: 19056393]
65. Flak JN, Solomon MB, Jankord R, Krause EG, Herman JP. Identification of chronic stress-activated regions reveals a potential recruited circuit in rat brain. *Eur J Neurosci* 2012;36(4):2547–55. [PubMed: 22789020]
66. Hinwood M, Tynan RJ, Day TA, Walker FR. Repeated Social Defeat Selectively Increases delta FosB Expression and Histone H3 Acetylation in the Infralimbic Medial Prefrontal Cortex. *Cereb Cortex* 2011;21(2):262–71. [PubMed: 20513656]
67. Laine MA, Sokolowska E, Dudek M, Callan SA, Hyytia P, Hovatta I. Brain activation induced by chronic psychosocial stress in mice. *Scientific Reports* 2017;7:11. [PubMed: 28127060]
68. Hasel P, Dando O, Jiwaji Z, Baxter P, Todd AC, Heron S, et al. Neurons and neuronal activity control gene expression in astrocytes to regulate their development and metabolism. *Nat Commun* 2017;8:15132. [PubMed: 28462931]
69. Sze Y, Gill AC, Brunton PJ. Sex-dependent changes in neuroactive steroid concentrations in the rat brain following acute swim stress. *J Neuroendocrinol* 2018;30(11).
70. Meffre D, Labombarda F, Delespierre B, Chastre A, De Nicola AF, Stein DG, et al. Distribution of membrane progesterone receptor alpha in the male mouse and rat brain and its regulation after traumatic brain injury. *Neuroscience* 2013;231:111–24. [PubMed: 23211561]
71. Handa RJ, Weiser MJ. Gonadal steroid hormones and the hypothalamo-pituitary-adrenal axis. *Front Neuroendocrinol* 2014;35(2):197–220. [PubMed: 24246855]
72. Seney ML, Huo Z, Cahill K, French L, Puralewski R, Zhang J, et al. Opposite Molecular Signatures of Depression in Men and Women. *Biological Psychiatry* 2018.
73. Goldwater DS, Pavlides C, Hunter RG, Bloss EB, Hof PR, McEwen BS, et al. Structural and functional alterations to rat medial prefrontal cortex following chronic restraint stress and recovery. *Neuroscience* 2009;164(2):798–808. [PubMed: 19723561]

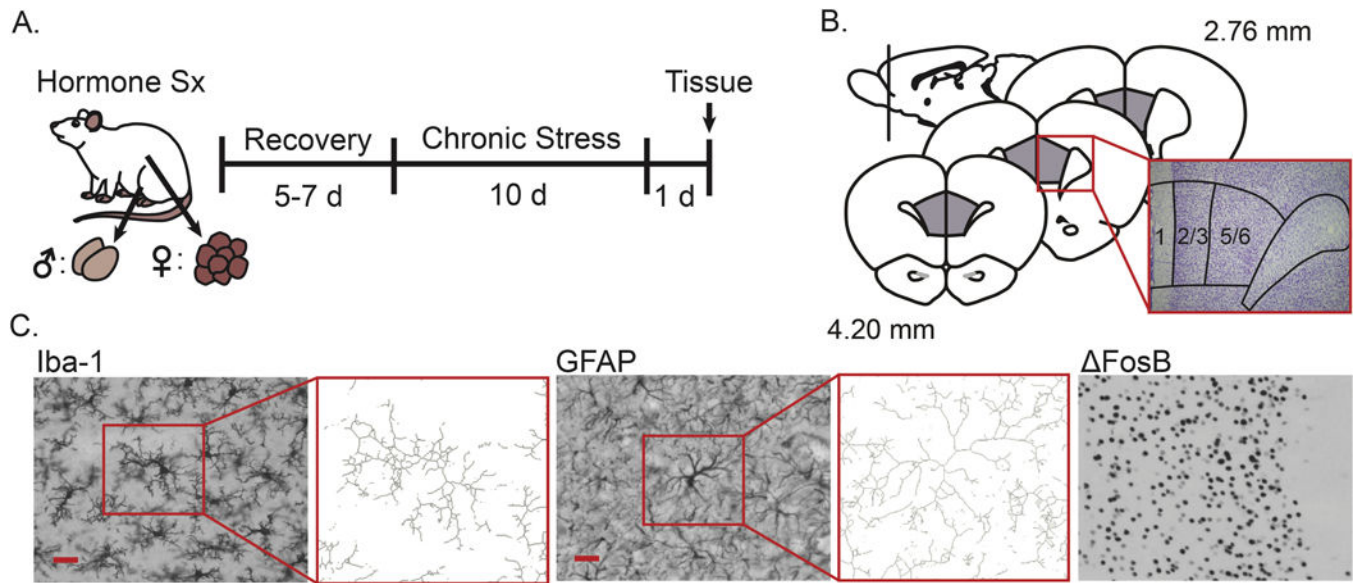


**Fig 1.**

Experimental design and histological analyses in prelimbic cortex. A. Male and female rats underwent either sham surgery or hormone manipulation (male: castration with or without hormone replacement, female: ovariectomy with or without hormone replacement), after which they were given 5–7 days to recover. Rats were then restrained for 3 hours/day over 10 days, or were left unhandled except for weighing every other day. Approximately 24 h after the final stressor, rats were euthanized and brains were collected, sectioned, and stained. Sx: Surgery. B. Prelimbic cortex was identified based on cytoarchitecture. C. Microglia (Iba-1) and astrocytes (GFAP) were visualized, and neuronal activation was inferred from FosB expressing cells. Microglial and astrocyte morphology were characterized using a standardized threshold technique (immunopositive area) and skeleton analyses (process complexity = z-normalized number of branch points + z-normalized branch length / 2). Scale bar = 25  $\mu$ m.

# MANIPULATION VERIFICATION

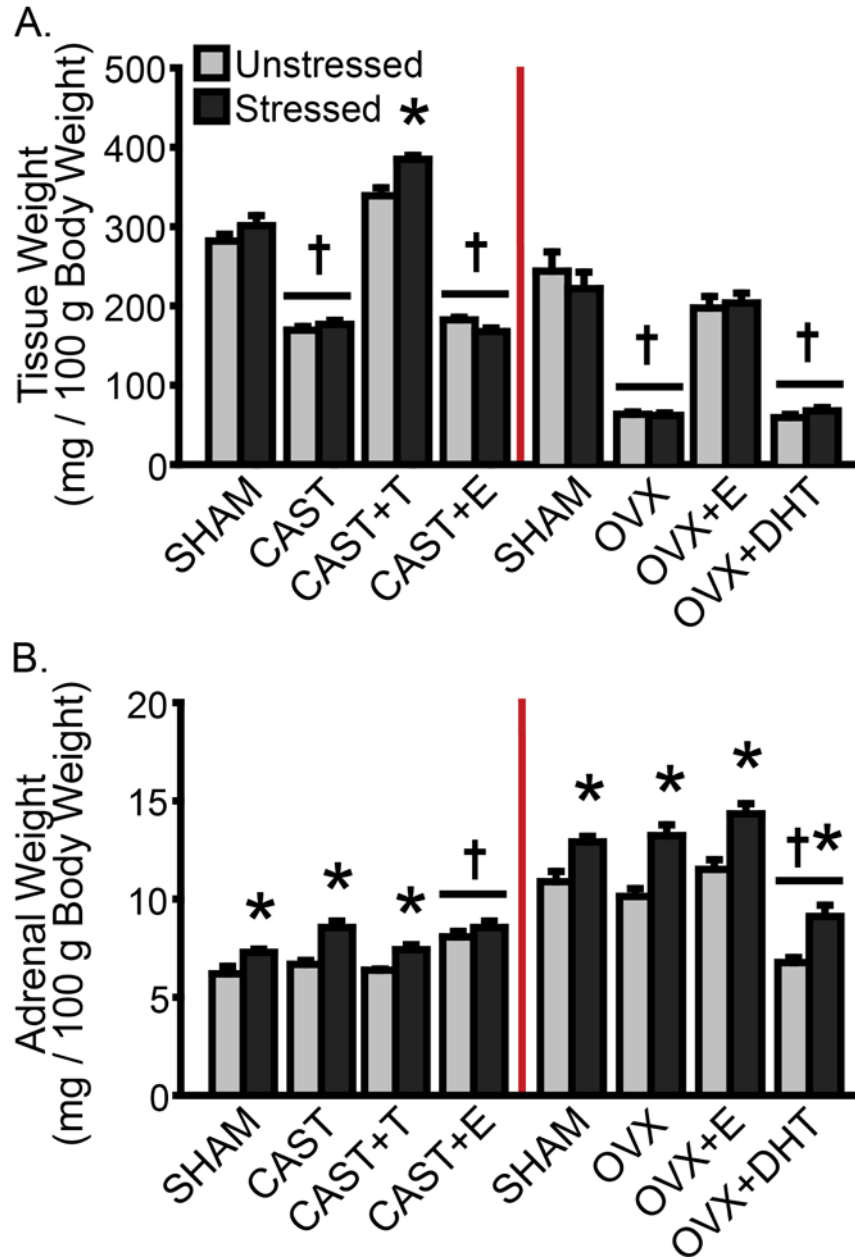


**Fig 2.** Effects of gonadectomy, hormone replacement, and stress on tissue weight in male and female rats. A. Data are displayed as mean BC/LA- (male, left) or uterine- (female, right) weight-to-body-weight ratios (tissue weight / 100g body weight). B. Adrenal weight-to-body-weight ratios (tissue weight / 100g body weight). CAST: Gonadectomized males without hormone treatment. OVX: Gonadectomized females without hormone treatment. +T: Treated with testosterone. +E: Treated with estradiol. +DHT: Treated with dihydrotestosterone. †p < .05 compared to same-sex unstressed SHAM group. \*p < .05

compared to same-hormone treatment unstressed group. Error bars indicate SEM. Number of animals per group: SHAM male (unstressed: 6, stressed: 6), CAST (unstressed: 8, stressed: 9), CAST+T (unstressed: 6, stressed: 5), CAST+E (unstressed: 6, stressed: 7), SHAM female (unstressed: 8, stressed: 9), OVX (unstressed: 7, stressed: 8), OVX+E (unstressed: 8, stressed: 8), OVX+DHT (unstressed: 8, stressed: 7).

### BASAL SEX DIFFERENCES

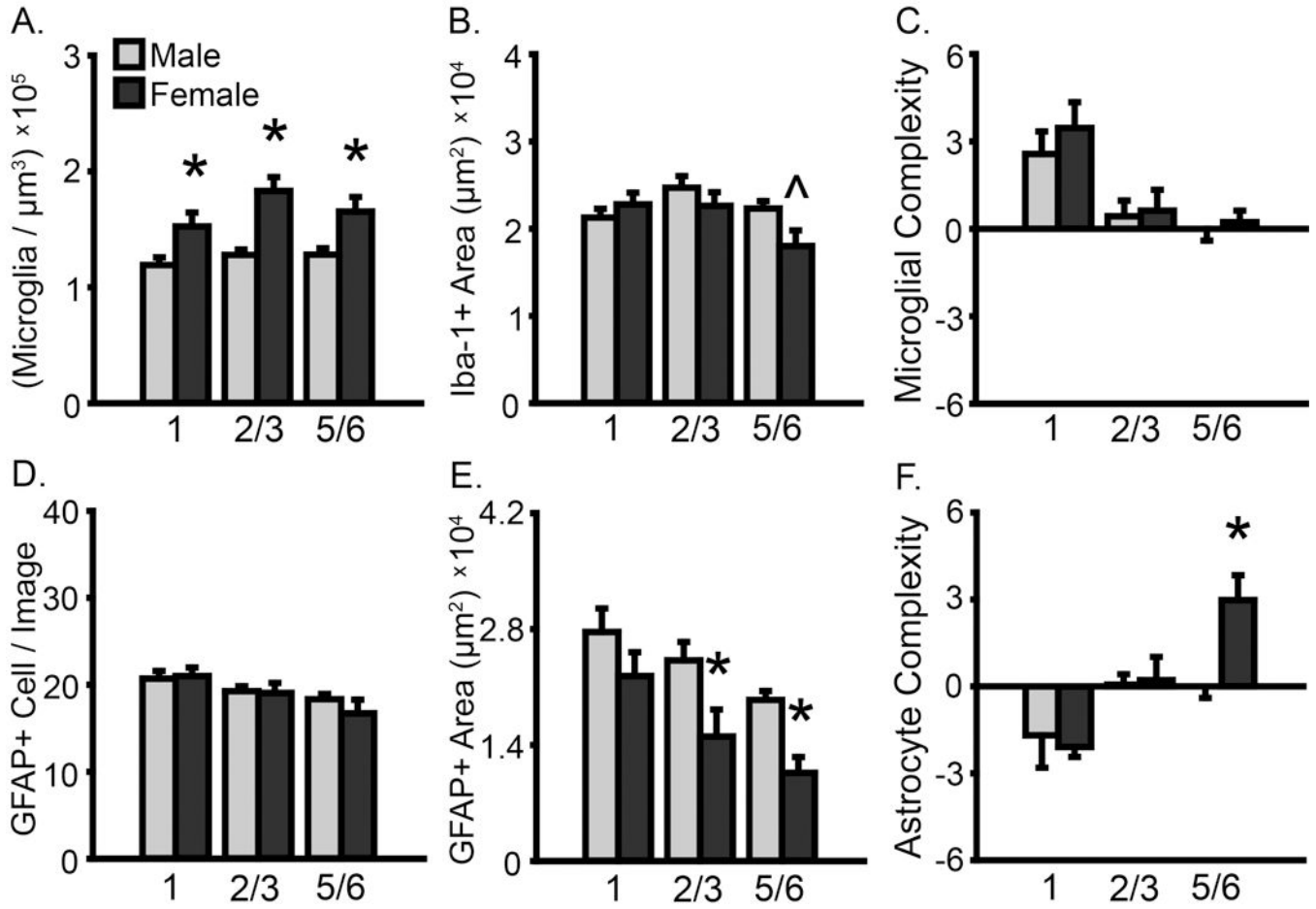


**Fig 3.** Basal sex differences in microglial and astrocyte number and morphology in prelimbic cortex. Sex differences in prelimbic cortex were examined in unstressed SHAM male and female rats. A. Total microglial density based on estimated volume. B. Iba-1+ area. C. Process complexity per microglia. Microglial density is greater in females compared to males. D. GFAP+ cells counted per image analyzed. E. GFAP+ area. F. Process complexity per GFAP+ cell. Astrocytic process coverage is heightened in males. \*p < .05 compared to unstressed SHAM males. X-axis labels represent layer (1, 2/3, 5/6). Error bars indicate SEM. Number of animals per group: SHAM male (unstressed: 6), SHAM female (unstressed: 7–8). Female outlier removed from microglial density (layer 1, *n* = 1) and area (all layers, *n* = 1) analyses.



**MALE: MICROGLIA**

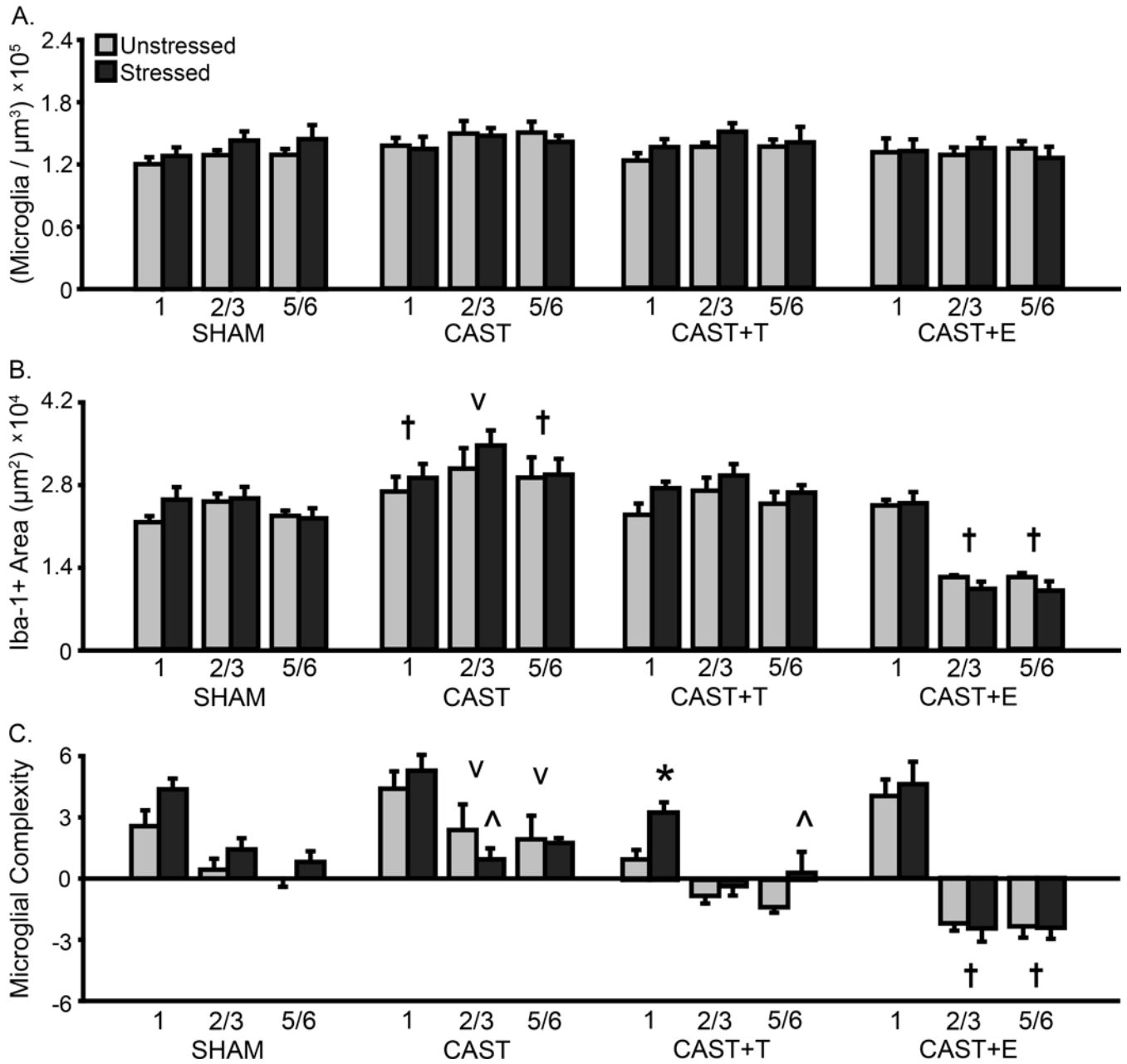


**Fig 4.** Layer-specific effects of gonadal hormones and stress on microglial density and morphology in prelimbic cortex in male rats. **A.** Total microglial density based on estimated volume. **B.** Total area of Iba-1+ material. The area of Iba-1+ material was greater in CAST males, and was reduced in layers 2/3 and 5/6 in CAST+E males compared to SHAM animals. **C.** Process complexity per microglia. Microglial complexity was increased in layers 2/3 and 5/6 in CAST males, and decreased in CAST+E as compared to SHAM males. Stress decreased microglial complexity in CAST males, and increased microglial complexity in CAST+T

males. CAST: Gonadectomized males without hormone treatment. +T: Treated with testosterone. +E: Treated with estradiol. † $p < .05$  compared to same layer SHAM group. † $p < .05$ , <sup>v</sup> $p < .10$  compared to same layer SHAM group. \* $p < .05$ , ^  $p < .10$  compared to same hormone condition unstressed group. X-axis labels represent layer (1, 2/3, 5/6). Error bars indicate SEM. Number of animals per group: SHAM male (unstressed: 6, stressed: 6), CAST (unstressed: 6–8, stressed: 6–9), CAST+T (unstressed: 6, stressed: 5), CAST+E (unstressed: 6, stressed: 7). CAST outlier removed from microglial complexity analysis (unstressed: layer 2/3,  $n = 1$ ).

**MALE: ASTROCYTES**

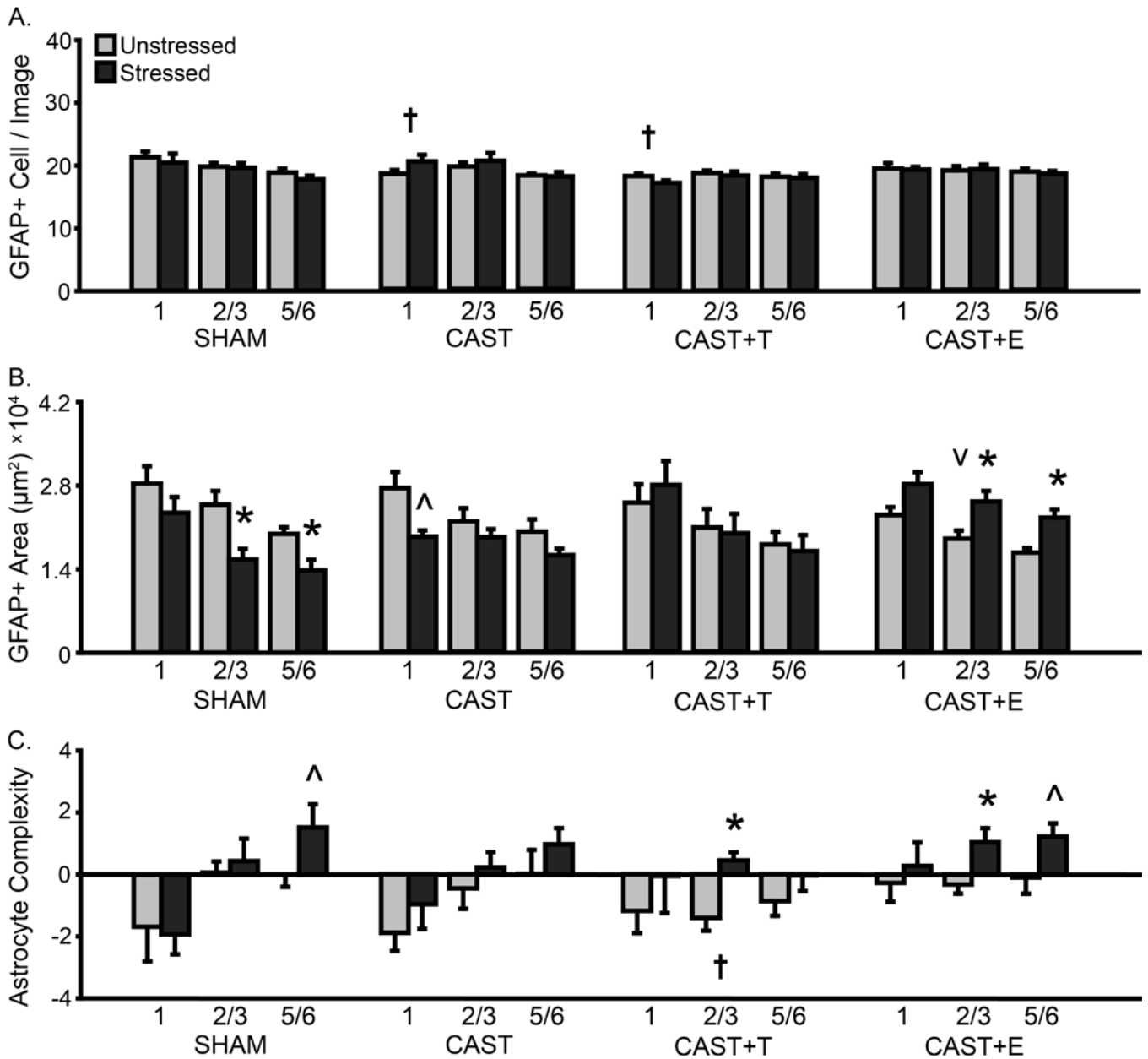


**Fig 5.** Layer-specific effects of gonadal hormones and stress on astrocyte counts and morphology in prelimbic cortex in male rats. A. Number of GFAP+ cells counted per image analyzed. The number of GFAP+ cells counted was reduced in layer 1 in CAST and CAST+T males compared to SHAM males. B. Total area of GFAP+ material. Stress decreased the area of astrocyte coverage in layers 2/3 and 5/6 in SHAM males and in layer 1 in CAST males, yet increased astrocyte area in layers 2/3 and 5/6 in CAST+E males. C. Process complexity per astrocyte. There was decreased process complexity in layer 2/3 in CAST+T compared to SHAM males. Stress increased astrocyte complexity in layer 5/6 in SHAM males, layer 2/3

in CAST+T males, and in layers 2/3 and 5/6 in CAST+E males. CAST: Gonadectomized males without hormone treatment. +T: Treated with testosterone. +E: Treated with estradiol. †p < .05, ††p < .10 compared to same layer SHAM group. \*p < .05, ^ p < .10 compared to same hormone condition unstressed group. X-axis labels represent layer (1, 2/3, 5/6). Error bars indicate SEM. Number of animals per group: SHAM male (unstressed: 6, stressed: 6), CAST (unstressed: 6–8, stressed: 6–9), CAST+T (unstressed: 6, stressed: 5), CAST+E (unstressed: 6, stressed: 7). CAST outlier removed from astrocyte area analysis (unstressed: layer 2/3,  $n = 1$ ; stressed: layer 1,  $n = 2$ , layer 2/3,  $n = 1$ ).

Author Manuscript

Author Manuscript

Author Manuscript

Author Manuscript

**MALE: CELL-CELL CORRELATION**

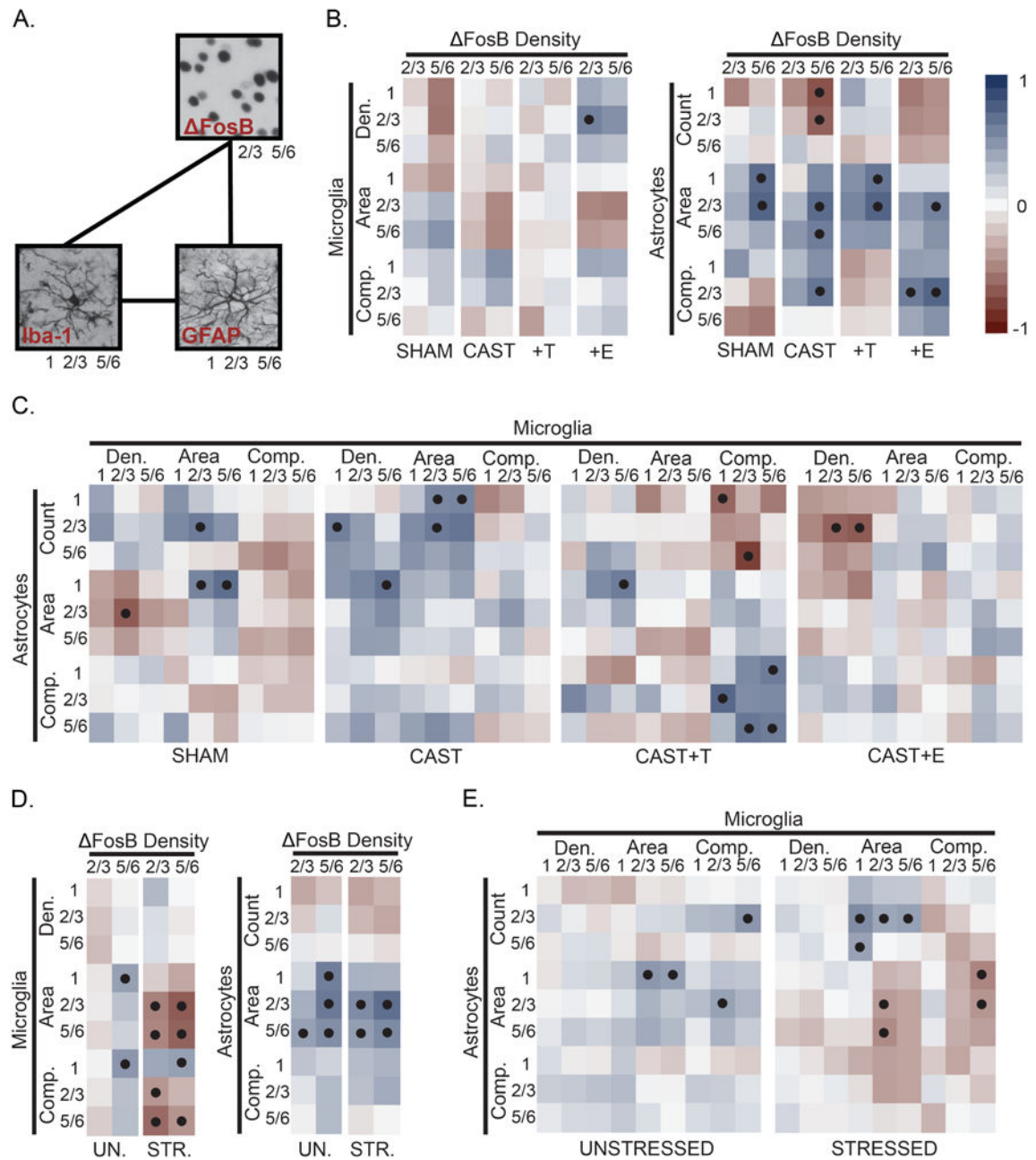


**Fig 6.** Hormone- and stress- effects on neuronal activity-glia, and microglia-astrocyte associations in prelimbic cortex in male rats. **A.** Main effects of hormone treatment and stress on associations between neuronal activity ( FosB expressing cells) and glia, alongside coupling of microglia-astrocyte measures were examined using Pearson’s correlation coefficients. **B.** There were relatively few strong associations between neuronal activity and measures of microglial density and morphology in males. However, CAST and CAST+E males exhibited an overall pattern divergent from SHAM and CAST+T males. In contrast, neuronal activity

was strongly associated with astrocyte morphology in males, regardless of hormone manipulation. C. Strong associations between microglial and astrocyte measures were relatively sparse, and this was unaltered by hormone manipulation. The overall pattern of these associations appears to be hormone-dependent; CAST and CAST+E males exhibit correlational patterns that differ from SHAM and CAST+T males. D. Stress increased neuronal activity-microglial coupling, yet had little effect on associations between neuronal activity and astrocyte morphology in males. E. Stress induced a pattern of negative microglia-astrocyte association. Positive (reds) and negative (blues) correlation coefficients are represented by matrix color. •  $p < .05$ . Layer noted as 1, 2/3, and 5/6. See Fig 4–5 and Supplementary Fig 2 for number of animals analyzed per group.

**FEMALE: MICROGLIA**

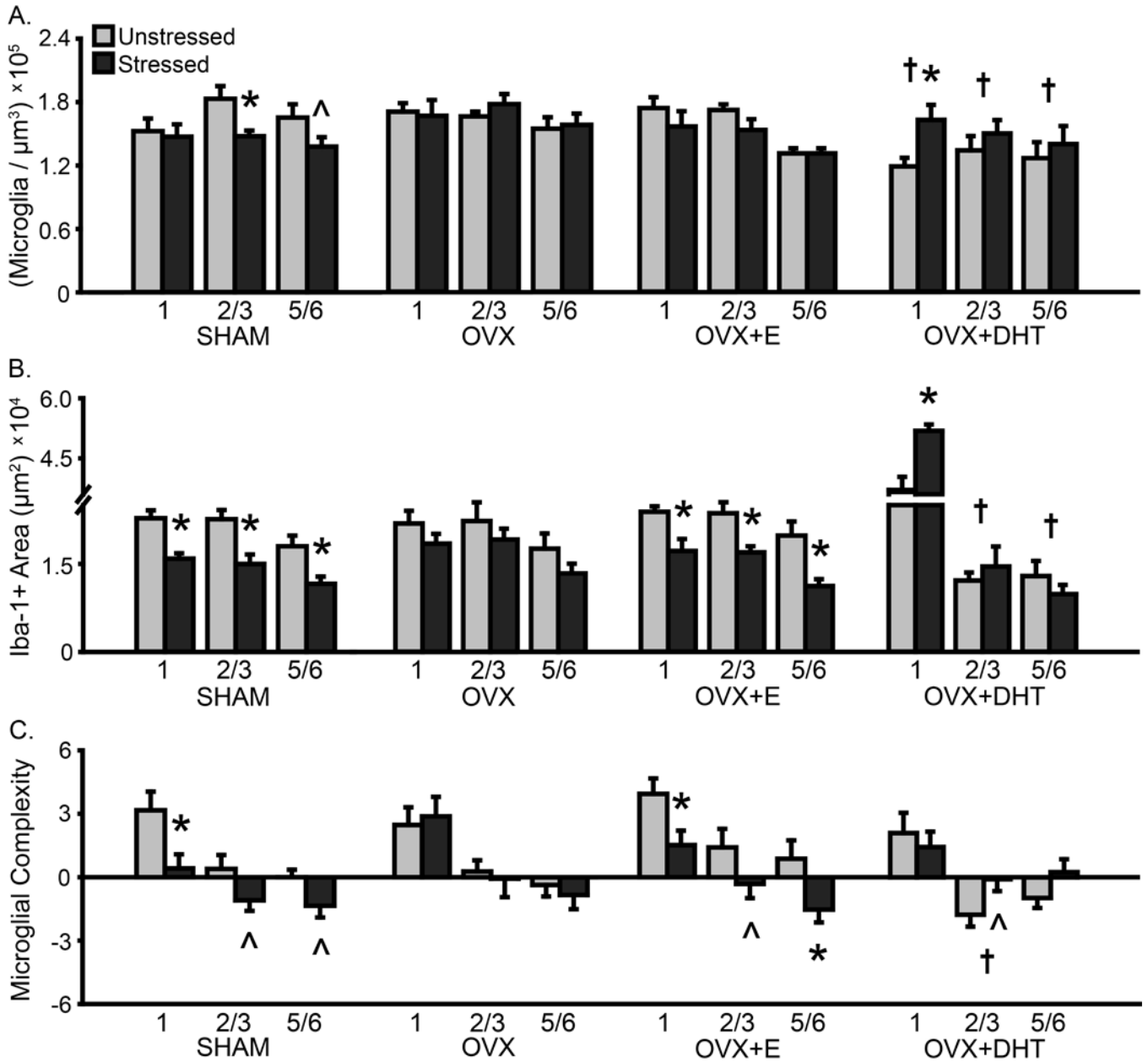


**Fig 7.** Layer-specific effects of gonadal hormones and stress on microglial density and morphology in prefrontal cortex in female rats. **A.** Total microglial density based on estimated volume. The density of microglia was reduced in OVX+DHT compared to SHAM females. Stress reduced microglial density in SHAM females yet increased this in OVX+DHT animals. **B.** Total area of Iba-1+ material. Stress reduced the area of microglial material in SHAM and OVX+E females across all layers, whereas treatment with DHT led to a stress-induced increase in Iba-1+ area in layer 1 in OVX females. **C.** Process complexity per microglia. There was decreased microglial complexity in layer 2/3 in OVX+DHT females. Stress

induced a tendency toward- or significantly- decreased microglial complexity in SHAM and OVX+E females. OVX: Gonadectomized females without hormone treatment. +E: Treated with estradiol. +DHT: Treated with dihydrotestosterone. † $p < .05$  compared to same layer SHAM group. \* $p < .05$ , ^  $p < .10$  compared to same hormone condition unstressed group. X-axis labels represent layer (1, 2/3, 5/6). Error bars indicate SEM. Number of animals per group: SHAM female (unstressed: 7–8, stressed: 8–9), OVX (unstressed: 7, stressed: 7–8), OVX+E (unstressed: 7–8, stressed: 7–8), OVX+DHT (unstressed: 8, stressed: 7). SHAM outlier removed from microglial density (unstressed: 1,  $n = 1$ ; stressed: 2/3,  $n = 1$ ) and area (unstressed: all layers,  $n = 1$ ; stressed: 1,  $n = 1$ ) analyses. OVX+E outlier removed from microglial density (unstressed: 2/3,  $n = 1$ ) and area (unstressed: 1,  $n = 1$ ; stressed: 2/3,  $n = 1$ ) analyses.



**FEMALE: ASTROCYTES**

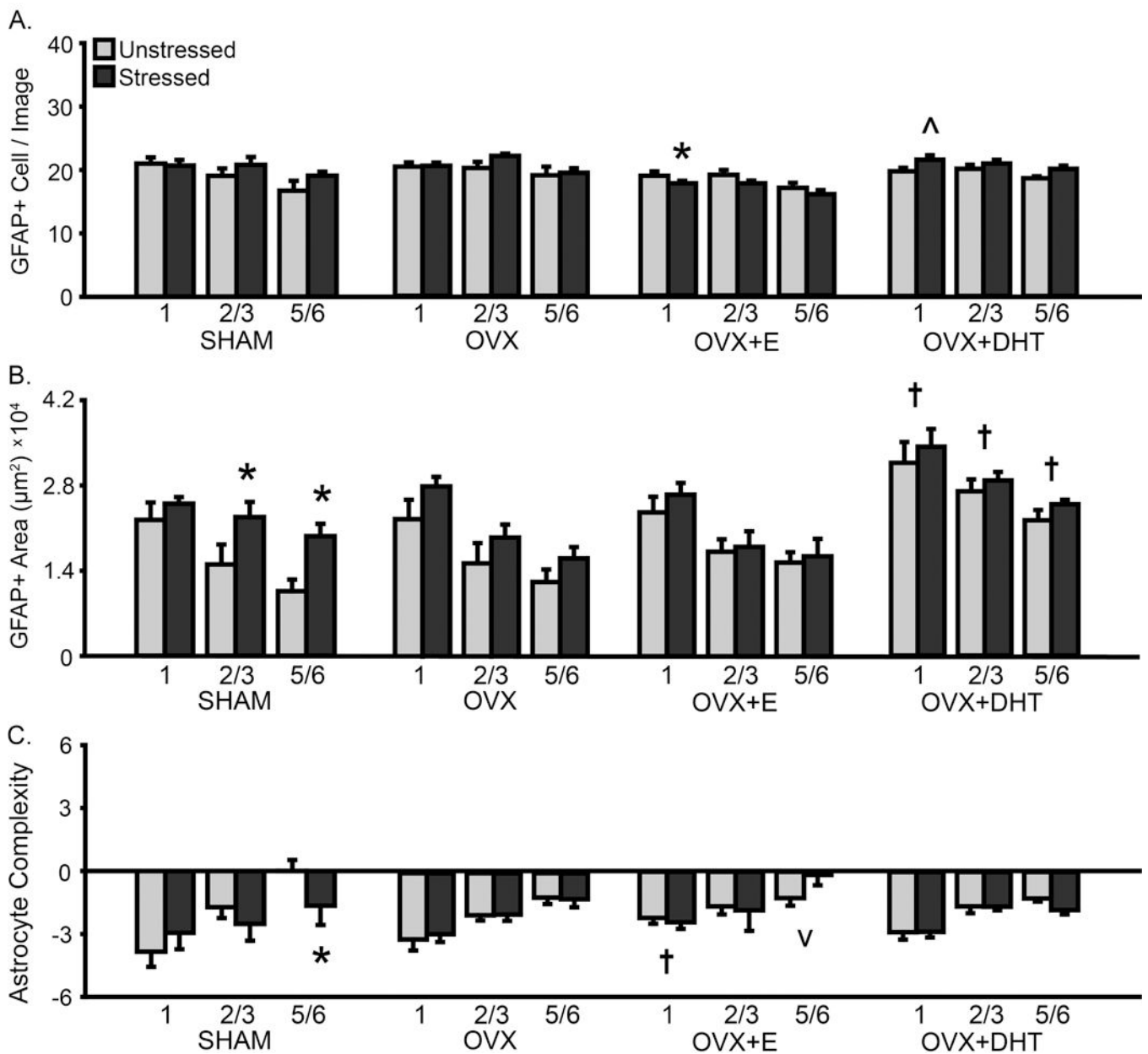


**Fig 8.** Layer-specific effects of gonadal hormones and stress on astrocyte counts and morphology in prelimbic cortex in female rats. A. Number of GFAP+ cells counted per image analyzed. B. Total area of GFAP+ material. Treatment with DHT increased GFAP+ area in OVX females. Stress increased the area of astrocyte coverage in layers 2/3 and 5/6 in SHAM females. C. Process complexity per astrocyte. Stress reduced astrocytic complexity in layer 5/6 in SHAM females. OVX: Gonadectomized females without hormone treatment. +E: Treated with estradiol. +DHT: Treated with dihydrotestosterone. †p < .05, † p < .10 compared to same layer SHAM group. \*p < .05, ^ p < .10 compared to same hormone

condition unstressed group. X-axis labels represent layer (1, 2/3, 5/6). Error bars indicate SEM. Number of animals per group: SHAM female (unstressed: 7–8, stressed: 7–8), OVX (unstressed: 7, stressed: 8), OVX+E (unstressed: 8, stressed: 8), OVX+DHT (unstressed: 8, stressed: 7). SHAM outlier removed from astrocyte area analysis (unstressed: 5/6,  $n = 1$ ; stressed: 1,  $n = 1$ ).

**FEMALE: CELL-CELL CORRELATION**

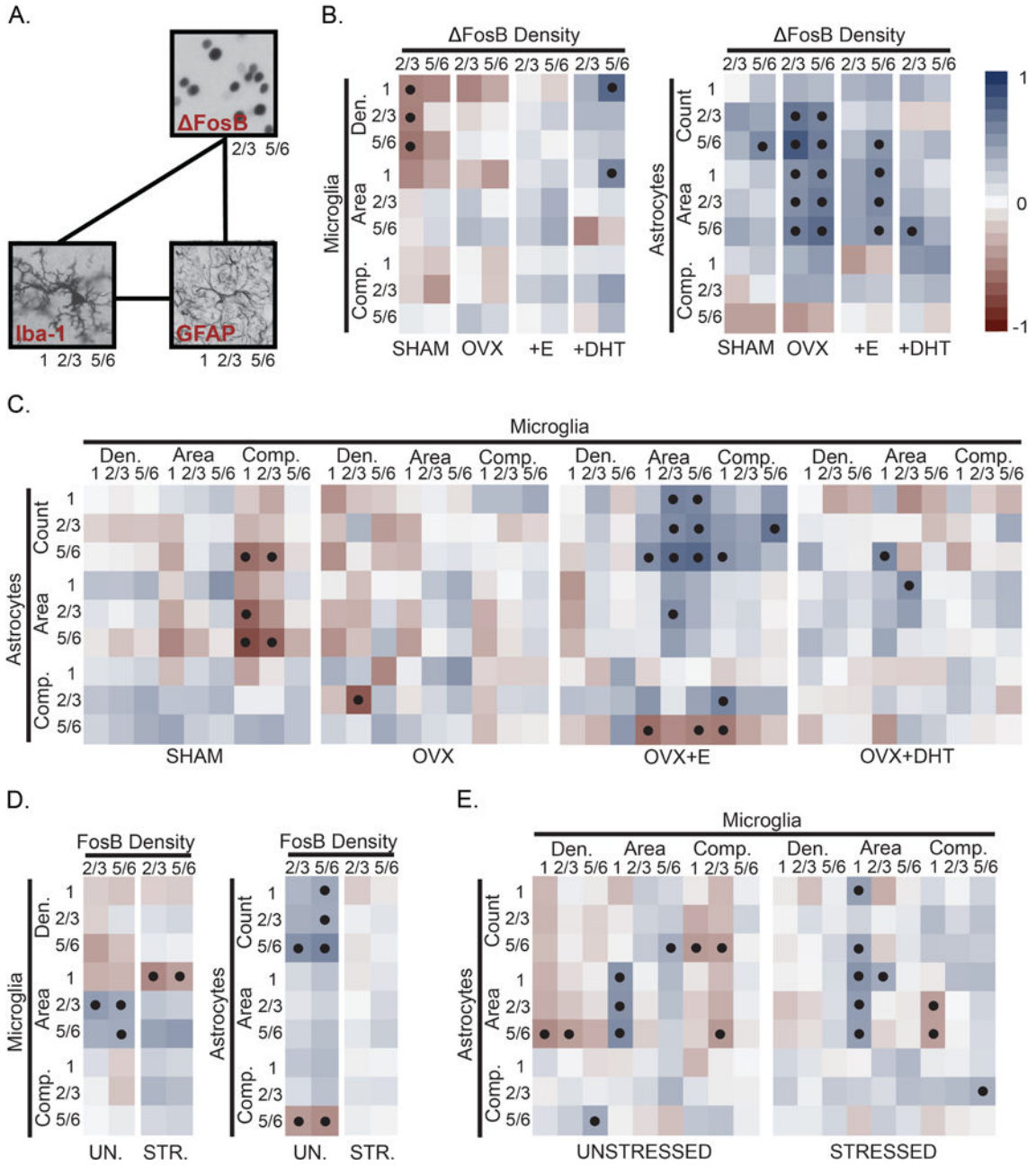


**Fig 9.** Hormone- and stress- effects on neuronal activity-glia, and microglia-astrocyte associations in prelimbic cortex in female rats. A. Similar to males, main effects of hormone treatment and stress on associations between neuronal activity ( FosB expressing cells) and glia, alongside coupling of microglia-astrocyte measures were examined using Pearson’s correlation coefficients in females. B. Measures of microglial density and morphology were weakly- or negatively- associated with neuronal activity in females. Hormone manipulation shifted this pattern, whereas treatment with DHT induced coupling between neuronal

activity and microglial measures. Neuronal activity was generally associated with astrocyte morphology in females; this relationship was strongest in OVX females. C. Measures of microglial and astrocyte morphology were negatively correlated in SHAM females. OVX reduced this association, whereas treatment with E strengthened connections between astrocyte number and microglial morphology. Associations between microglia and astrocytes were, overall, similar in OVX and OVX+DHT animals. D. Stress shifted patterns of neuronal activity-microglial coupling, and reduced neuronal activity-astrocyte associations. E. Measures of microglial and astrocyte morphology were, generally, negatively associated. Stress weakened or reversed this pattern. Positive (red tone) and negative (blue tone) correlation coefficients are represented by matrix color. •  $p < .05$ . Layer noted as 1, 2/3, and 5/6. See Fig 7–8 and Supplementary Fig 2 for number of animals analyzed per group.

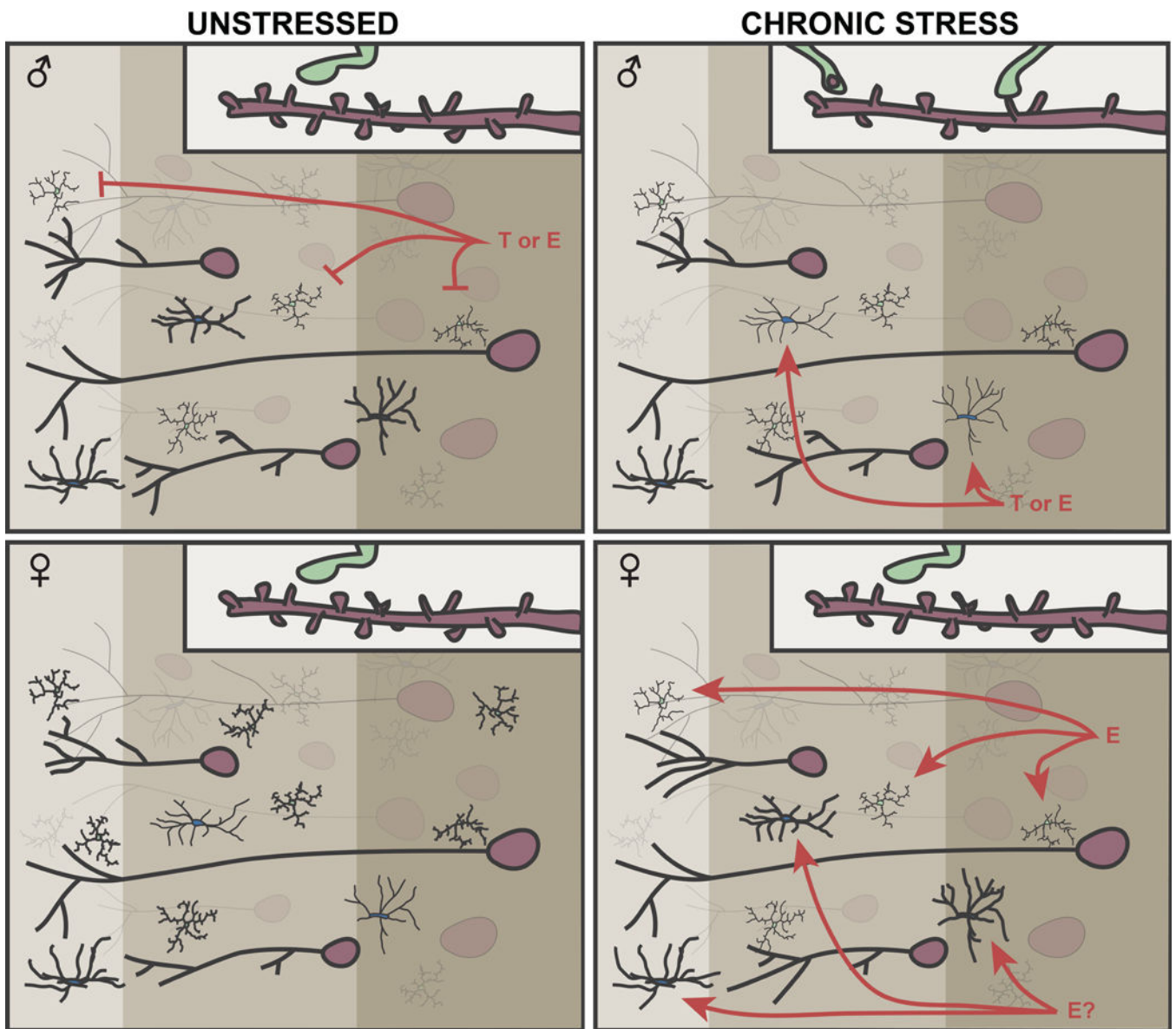


**Fig 10.**

Sex differences in- and sex dependent stress effects on- cellular architecture across mPFC. Left panel. Males show more complex dendritic arbors in layers 1 and 2/3 in mPFC compared to females. Likewise, astrocyte structure is more complex in layers 2/3 and 5/6. Activated microglia can prune synapses and remodel dendritic architecture. In line with this, males show reduced microglial density or activation state across all layers compared to females. Top left. In males, T and/or E regulate basal aspects of microglial morphology across mPFC. Top right: Chronic stress effects on neuronal morphology differ by dendritic location and cortical layer. Stress induces apical – but not basilar – dendritic retraction and spine loss in layers 1 and 2/3 in males (44, 62), yet has little effect on dendritic arborization in layer 5/6 (73). Perhaps mediating these effects, chronic stress increases microglia-neuron contact and microglial engulfment of dendritic spines near layers 1 and 2/3 – but not layer 5/6, suggesting layer-specific microglia-mediated neuronal remodeling (12). Shifts in

microglial morphology were not detected in this study. Astrocytes undergo stress-induced atrophy in layers 2/3 and 5/6; this appears to be mediated – in part – by either T or E. Bottom left. Gonadal hormones do not regulate basal microglial or astrocyte morphology in mPFC in females. Bottom right. Chronic stress has either no effect on- or increases dendritic complexity in layers 2/3 in females. This may be due to a significant decrease in microglial density/activation and – in turn – reduced microglial maintenance or pruning across mPFC. Stress-induced neuronal and microglial remodeling is estradiol dependent. Chronic stress leads to astrocytic growth or reorganization (i.e. increased process complexity) across mPFC. As ovariectomy or hormone replacement disrupts stress effects on astrocyte morphology, it is possible that gonadal hormones regulate aspects of stress-induced astrocyte remodeling in females. Light tan: layer 1, medium tan: layer 2/3, dark tan: layer 5/6. Purple: pyramidal neurons, blue: astrocytes, green: microglia.